NMR in Biomedicine

Investigating Lipids as a Source of Chemical Exchange-Induced MRI Frequency Shifts

Journal:	*NMR in Biomedicine*
Manuscript ID	NBM-15-0320.R2
Wiley - Manuscript type:	Special Issue Research Article
Date Submitted by the Author:	n/a
Complete List of Authors:	Shmueli, Karin; University College London, Department of Medical Physics and Biomedical Engineering; National Institutes of Health, Advanced MRI Section, Laboratory of Functional & Molecular Imaging, National Institute of Neurological Disorders & Stroke Dodd, Stephen; National Institutes of Health, Laboratory of Functional & Molecular Imaging, National Institute of Neurological Disorders & Stroke van Gelderen, Peter; National Institutes of Health, Advanced MRI Section, Laboratory of Functional & Molecular Imaging, National Institute of Neurological Disorders & Stroke Duyn, Jeff; National Institutes of Health, Advanced MRI Section, Laboratory of Functional & Molecular Imaging, National Institute of Neurological Disorders & Stroke
Keywords:	Chemical Exchange, Chemical shift imaging, Multilamellar Lipid Vesicles, Dioxane, Exchange-Induced Resonance Frequency Shifts, Phospholipids

Investigating Lipids as a Source of Chemical Exchange-Induced MRI Frequency Shifts

K. Shmueli[1,2], S. J. Dodd[3], P. van Gelderen[1] and J. H. Duyn[1]

1. Advanced MRI Section, Laboratory of Functional & Molecular Imaging, National Institute of Neurological Disorders & Stroke, National Institutes of Health, USA
2. Department of Medical Physics & Biomedical Engineering, University College London, UK
3. Laboratory of Functional & Molecular Imaging, National Institute of Neurological Disorders & Stroke, National Institutes of Health, USA

Word Count

5,312 words

Sponsors

This research was supported by the intramural research program of the National Institute for Neurological Disorders and Stroke at the National Institutes of Health.

Karin Shmueli is partly supported by the Engineering and Physical Research Council grant EP/K027476/1.

Keywords

Chemical Exchange

Exchange-Induced Resonance Frequency Shifts

Chemical shift imaging

Dioxane

Multilamellar Lipid Vesicles

Phospholipids

Abbreviations:

BSA	bovine serum albumin
CSI	chemical shift MR imaging
d	dioxane concentration
dmf	dioxane molar fraction
f_e	Exchange-induced frequency shift
$f_{w\text{-}d}$.	Additional interaction-induced water frequency shift relative to dioxane frequency shift
GalCer	galactosylceramides
GC	Galactocerebroside
GM	gray matter
MLVs	multilamellar vesicles
MT	magnetization transfer
NH	amide
OH	hydroxyl
PBS	phosphate-buffered saline
POPC	phospholipid: 16:0-18:1 PC, 1-palmitoyl-2-oleoyl-*sn*-glycero-3-phosphocholine
R	peak area ratio (dioxane:water) should be proportional to the relative concentration of dioxane to water
ROI	region of interest
SNR	signal-to-noise ratio
TSP	3-(trimethylsilyl)-propionic acid-d_4 sodium salt, also called Sodium 3-(trimethylsilyl)-propionate-2,2,3,3-d_4 or 2,2,3,3,-tetradeutero-3-trimethylsilylpropionic acid
w	water concentration
WM	white matter
wmf	water molar fraction

Abstract:

While magnetic susceptibility is a major contributor to NMR resonance frequency variations in human brain, a substantial contribution may come from chemical exchange of protons between water and other molecules. Exchange-induced frequency shifts f_e have been measured in tissue and protein solutions but relatively lipid-rich white matter (WM) has a larger f_e than gray matter, suggesting that lipids could contribute. Galactocerebrosides (GC) are a prime candidate as they are abundant in WM and susceptible to exchange. To investigate this, f_e was measured in a model of WM lipid membranes in the form of multilamellar vesicles (MLVs), consisting of a 1:2 molar ratio of GC and phospholipids (POPC), and in MLVs with POPC only. Chemical shift imaging with 15% volume fraction of dioxane, an internal reference whose protons are assumed not to undergo chemical exchange, was used to remove susceptibility-induced frequency shifts in an attempt to measure f_e in MLVs at several lipid concentrations. Initial analysis of these measurements indicated a necessity to correct for small unexpected variations in dioxane concentration due to its effect on the water frequency shift. To achieve this, actual dioxane concentration was inferred from spectral analysis and its additional contribution to f_e was removed through separate experiments which showed that the water-dioxane frequency shift depended linearly on the dioxane concentration at low concentrations with a proportionality constant of –0.021 ± 0.002 ppb/mM in agreement with published experiments. Contrary to expectations and uncorrected results, for GC+POPC vesicles, the dependence of the corrected f_e on GC concentration was insignificant (0.023 ± 0.037 ppb/mM; $r^2 = 0.085$, $p>0.57$), while for the POPC-only vesicles a small but significant linear increase with POPC concentration was found: 0.044 ± 0.008 ppb/mM ($r^2 = 0.877$, $p<0.01$). These findings suggest that the non-susceptibility contribution of lipids to frequency contrast in WM may be small.

Introduction:

Gradient-echo MR frequency images are increasingly utilized because they provide high contrast that is complementary to conventional magnitude image contrast. Magnetic susceptibility is widely accepted as a major source of this tissue frequency contrast (1-3). In addition, recent measurements in fixed human and fresh pig brain tissues (4) show a substantial (and opposing) contribution to white-gray matter (WM-GM) frequency contrast from chemical exchange of protons between water and off-resonance molecular sites. Studies in protein solutions (5,6) also found a positive exchange-induced frequency shift (f_e) that was directly proportional to the concentration of bovine serum albumin (BSA) protein. On the basis of these protein studies, f_e contrast in brain tissue has been attributed to protons exchanging between water and protein amide (NH) and hydroxyl (OH) groups (6).

However, we cannot assume that proteins are the sole cause of the greater f_e observed in WM than in GM (4) given that both i) WM contains much less protein than GM (as a percentage of dry mass) (7) and ii) WM contains approximately 1.7 times the total lipid content of GM (as a percentage of dry mass) (7). The fact that the relatively lipid-rich WM has a larger f_e than GM suggests that there may be sites of exchange in lipids that contribute to the observed exchange-induced frequency shifts.

To begin to investigate whether lipids cause exchange-induced frequency shifts we chose to focus specifically on cerebrosides because they are a major component of human WM, constituting approximately 20% of the total lipid weight (7,8). Even more relevant for a potential cause of WM-GM f_e contrast, cerebrosides show the largest WM-GM difference of all the lipids, and are over three times more abundant in human WM than GM (7,8). Cerebrosides are ceramide-based glycosphingolipids (9-11) whose head groups consist of a single hexose sugar residue, with galactosylceramides (GalCer) or galactocerebrosides (GC) being most common in the central nervous system (12,13). Another reason why cerebrosides are a good

candidate for chemical exchange is that their head groups have several OH groups exposed at the surface of phospholipid cell membranes (14,15). These lipids have also been shown to cause large magnetization transfer (MT) effects that have been attributed to chemical exchange based on their pH-dependence (14).

Therefore, we tested the hypothesis that cerebrosides cause f_e, using an *in-vitro* model for WM cell membranes to investigate whether cerebrosides could contribute to the WM-GM f_e contrast in brain tissue.

Our chosen reference substance, dioxane, is known to affect the water frequency shift (16-19). Therefore, we kept the concentration of dioxane constant throughout our lipid experiments. We also set out to measure any dioxane-induced water frequency shifts separately in water/dioxane mixtures in the same experimental setup and incorporated any observed effects into our analysis of the lipid experiments.

Methods:

Choice of Lipids

To measure any f_e due to cerebrosides, a single-slice chemical shift MR imaging (CSI) experiment was performed in multi-lamellar vesicle samples containing several different concentrations of cerebrosides (GC). Multi-lamellar vesicles (MLV) are an authentic model for white matter; their onion-like structure closely resembles the multiple lipid bilayers of the myelin sheath on electron microscopy (20). However, because pure cerebrosides are highly insoluble in water and have a very high melting (gel to liquid crystalline) phase transition temperature (12,13) compared to other membrane lipids, they do not form stable multi-lamellar vesicles in aqueous solvents. For this reason, a phospholipid (16:0-18:1 PC, 1-palmitoyl-2-oleoyl-*sn*-glycero-3-phosphocholine, POPC), which is equivalent to naturally occurring

phosphatidylcholine, was included in all the lipid samples. A constant 2:1 POPC:GC molar ratio was chosen to approximate the phospholipid to glycolipid ratio in human WM (7,8,14).

To investigate whether cerebrosides led to exchange-induced frequency shifts, MLVs were made containing a range of cerebroside concentrations similar to those found in human WM. To test whether any observed exchange-induced frequency was caused by POPC, a control experiment was carried out using an identical setup but substituting pure POPC for cerebrosides to match the total lipid concentrations in each of the MLV samples.

Choice of Reference Chemical:

As in previous experiments (4,5), 1,4 dioxane was used as a reference chemical whose protons are assumed not to exchange with macromolecules. Dioxane was chosen over TSP (3-(trimethylsilyl)-propionic acid-d_4 sodium salt, also called Sodium 3-(trimethylsilyl)-propionate-2,2,3,3-d_4 or 2,2,3,3,-tetradeutero-3-trimethylsilylpropionic acid), which has also been used as a reference chemical in exchange experiments (4,6), because TSP has been found to interact slightly with macromolecules and has a chemical shift that varies with pH (21) suggesting that its protons do undergo chemical exchange with macromolecules (16). Dioxane, on the other hand, has been used as a reference in protein (5) and tissue experiments (4,22) and has been reported as an appropriate reference for proteins (21).

Prior to scanning, dioxane was added to all the lipid MLV samples as well as the surrounding phosphate-buffered saline (PBS) (see Fig. 1). Because local susceptibility-induced frequency shifts in a given voxel are identical for both water and dioxane protons, f_e can be measured by subtracting the dioxane frequency from the water frequency in every voxel; see Shmueli et al. (4) for theory. This relies on a key assumption that the frequency shift of the dioxane reference proton signal is only affected by susceptibility differences. Because recent work has highlighted that the frequency of water is affected by the dioxane concentration (16), we took care to keep

the dioxane concentration constant in all the MLV samples and the surrounding PBS. This was achieved by adding dioxane to all the samples at 15% volume ratio (i.e. 15% volume dioxane:volume PBS) at the final stage just before MR imaging. This concentration (15% v/v) was chosen to be high enough to provide sufficient SNR for dioxane peak detection within each CSI voxel (c.f. Luo et. al. (5)) and much lower than in (4) in an attempt to reduce systematic errors due to any unforeseen interactions. Each MLV sample (that had been rehydrated with 0.5 ml PBS – see below) had 75 µl of dioxane added and was thoroughly mixed. 7.5 ml of dioxane was mixed with 50 ml of PBS to make the solution used to fill the large outer tube.

Ultimately, regions of interest were drawn on maps of the exchange-induced frequency shift to allow calculation of any effect of increasing the cerebroside or POPC concentration on the measured f_e.

Preparation of Lipid MLV samples:

Stock solutions of lipids (16:0-18:1 PC 760.08 g/mol and total porcine brain cerebrosides - predominant species: 812.25 g/mol, average: 781.95 g/mol, Avanti Polar Lipids Inc., AL, USA), in chloroform for POPC and 2:1 chloroform: methanol for the cerebrosides were combined to achieve the desired range of lipid concentrations and molar ratio (2:1 POPC:GC). Six concentrations (shown Table 1 and in Figures 1b and 1h) were chosen to cover the range found in human WM and GM (7,8). The solvents were removed by slow evaporation under a vacuum, leaving a thin film of lipid. To form multi-lamellar vesicles (MLVs), the lipid films were rehydrated in equal volumes (0.5 ml) of heated (~75°C) phosphate-buffered saline (PBS) with 5 freeze-thaw cycles as in Kucharczyk et al. (14). The high temperature was needed because of the high cerebroside melting (gel to liquid crystalline) phase transition temperature (~70-90°C) (12,13). Freezing was achieved by immersing the sample vials in liquid Nitrogen, and thawing

was accomplished by immersing the vials in a water bath at approximately 75°C for 5 minutes. In each cycle, all samples were thoroughly vortexed for 1 minute after thawing.

Once prepared, dioxane, 15% v/v, was added to each MLV sample as well as the surrounding PBS taking care to mix thoroughly. Each MLV sample was transferred into a 5-mm diameter NMR tube (Wilmad Labglass, NJ, USA) and these smaller tubes (six tubes and an MLV 'control' tube – see below) were mounted into two PVC tube-holders designed to align and space the tubes regularly within a larger 25 mm-diameter NMR tube. The large outer NMR tube was filled with PBS (+15% dioxane v/v) to a level higher than that of all the lipid samples. In the GC experiment, a tube was filled with POPC MLVs at a concentration of 54 mM. Similarly, in the POPC experiment, a tube was filled with GC MLVs at a concentration of 18 mM GC (i.e. 54 mM total lipid). These extra tubes were intended as 'controls' in an attempt to allow cross-referencing between the different experiments.

Chemical Shift MR Imaging (CSI):

Single-slice chemical shift MR imaging (CSI) was performed using a 600 MHz vertical bore spectrometer (Bruker, Biospin) fitted with a birdcage radiofrequency (RF) coil of 30 mm internal diameter. The acquisition frequency was centered on the water peak prior to and after manual shimming before scanning. The CSI slice had 202 x 202 x 300 μm voxels and a matrix size of 124 x 124. The acquisition had a 45° flip angle and a spectral width of 10 kHz (100 μs per point) with 1024 time points and a delay of 1.57 ms before acquisition (to accommodate the RF pulse duration and phase encode gradients). The repetition time was 1 s and the total acquisition time was 4 hours, 16 minutes and 16 s. The bandwidth of the slice-selective RF pulse was 6.6 kHz. All scans were performed at stable room temperature and after the lipid samples had equilibrated to room temperature. This is important because chemical exchange rates are strongly dependent on temperature therefore exchange-induced frequency shifts are

expected to be influenced by temperature (23). The temperature in the scanner bore, close to the sample, was recorded throughout the scans. Across all experiments, the temperature ranged between 290.10 and 291.77°K) and varied by less than 0.1°K (or 0.2°K for the repeated GC measurement) within each experiment.

Data acquisition was repeated after 25 and a half hours (for the experiment with different GC concentrations) (GC repetition 2) to check the stability of the MLVs and the reproducibility of the results. For this reason a second control (POPC) experiment (POPC 2) was also done with new MLV lipid samples and PBS and identical parameters to the first POPC (POPC 1) and GC experiments. This second POPC experiment (POPC 2, repetition 1), was repeated after 18 hours (POPC 2, repetition 2) (with a slightly different slice position and a different shim) and again after 23 hours (POPC 2, repetition 3) with TR increased from 1s to 2s, flip angle increased from 45° to 60° and gradient spoiler strength increased from 15% to 40% to increase SNR and rule out any contributions from unwanted coherences.

Water-Dioxane Experiment:

To allow for the potential correction of f_e for unintended small variations in dioxane concentration, we attempted to quantitatively assess the contribution from the previously reported relationship between the water frequency shift and the dioxane concentration (16-19). For this purpose, we performed an experiment similar to the MLV experiments described above by varying the relative concentrations of water and dioxane only (with no lipids).

The same NMR tube configuration and spacers were used but were filled only with water and dioxane at concentrations given in Table 2. These concentrations were chosen to cover the range expected in our lipid experiments as well as to reproduce the results in (16,18). CSI experiments were performed with identical acquisition parameters to those described above. The data were

also analysed exactly as described below but now assuming that any apparent frequency shifts $f_{w\text{-}d}$ were due to interactions between dioxane and water as described in (16-19).

Data Analysis

Primary analysis was geared towards estimating f_e from the spectral shift between water and dioxane peaks as a function of lipid concentration in the GC+POPC and POPC samples. Additional analysis was performed to estimate the precise dioxane concentration, in order to correct the primary results for small variations in the dioxane concentration that may have affected f_e. For this purpose, the water/dioxane experiment was analyzed for the dependence of the water frequency shift on the dioxane concentration inferred from the dioxane spectral intensity. The primary analysis closely followed that in Shmueli et al (4). The first 512 points (51.2 ms) of the raw, time domain data were selected for further analysis because most of the signal had decayed by the end of that time window. To select separate water and dioxane signals, the data were Fourier transformed into the frequency (spectral) domain and band-pass filters were placed around the water and dioxane peaks. The filters had a width of 550 Hz and cosine transition zones of widths 120 Hz. The central 64 points of the filtered spectra were Fourier transformed back into the time-domain and a 2-D spatial Fourier transform was performed to give separate water and dioxane magnitude and phase images over time.

In each voxel, the water-dioxane phase difference was fitted over time using least-squares linear regression to obtain f_e as the gradient of the linear fit divided by 2π. The fitting algorithm was designed to be effective in unwrapping the phase difference in each voxel over time. To ensure that the phase difference was fit only over time points and in voxels at which it had a sufficient signal-to-noise ratio (SNR), low-signal voxels in air bubbles and glass tube walls were excluded from the fit by thresholding the water magnitude image, and only time points having a water

magnitude SNR greater than 10 were included in the fit. This meant that the standard deviation of the noise in the phase image at each time point included in the fit was less than 0.1 radians because the noise in the phase image is equal to $1/SNR_{mag}$ (24).

The fit results were used to create maps of the exchange-induced frequency shift, f_e, for each experiment (see Figures 1a and 1g). Regions of interest (ROIs) were placed on these f_e maps to allow calculation of any effect of increasing the cerebroside or POPC concentration on the measured f_e. To calculate the mean and standard deviation of f_e for each lipid concentration, ROIs were drawn in the MLV-containing NMR tubes and surrounding fluid. The ROIs were drawn on the magnitude (water) image at TE = 9.57 ms, taking care to mask out air bubbles, glass tube walls and any other areas of low signal. The mean and standard error of f_e were recorded for each ROI. Any apparent f_e in the PBS ROI was subtracted from the raw f_e map to correct for any frequency shifts caused by inaccurate centering of the spectral band-pass filters on the resonance peaks in the CSI data. This step relied on the assumption that there is no exchange (and therefore zero f_e) in the PBS due to the absence of lipids or other off-resonance exchanging protons.

Correction of the primary analysis of lipid samples for small variations in dioxane concentration proceeded as follows. As the frequency shift between water and dioxane resonance ($f_{w\text{-}d}$) depends on the relative concentration of water and dioxane (16-19) we first estimated the relative dioxane/water concentration for each lipid concentration using their peak area ratio. The area under a resonance peak in a spectrum should be directly proportional to the number of protons resonating at that chemical shift and to the concentration of that chemical species (25). Therefore, the peak area ratio (R) should be proportional to the relative concentration of dioxane and water. Because there are 8 protons per dioxane molecule and 2 per water molecule, the relative concentration of dioxane (d) to water (w)

$$d/w = R/4 \qquad [1]$$

Therefore

$$R = 4(1/wmf - 1) \quad [2]$$

where wmf is the water molar fraction = w /(w+d).

In all experiments, the peak area ratio was measured by integrating the amplitudes (25) of the central 64 points of the filtered water and dioxane spectra in each voxel and taking the ratio of these peak areas. All further calculations were based on the mean peak area ratios inside each of the ROIs defined as described above.

The measured frequency shifts in the water-dioxane experiment $f_{w\text{-}d}$ were found to vary linearly with the measured peak area ratio (see Fig. 2c). Therefore, this best-fit linear relationship between $f_{w\text{-}d}$ and the peak area ratio from the water-dioxane experiments was used to predict an expected water-dioxane frequency shift $f_{wd\text{-}pred}$ (e.g. Figures 1e and 1k) from the measured peak area ratio for each ROI in the lipid experiments (e.g. Figures 1d and 1j). Finally, the residual $f_{wd\text{-}pred}$ values – relative to the intercept of the best-fit line of $f_{wd\text{-}pred}$ against lipid concentration (e.g. Figures 1e and 1k) – were subtracted from the original lipid f_e values in the same ROI (e.g. Figures 1c and 1i) to obtain the corrected lipid f_e values (Figures 1f and 1l).. The gradient and r^2 values of the best-fit lines to these corrected f_e values against lipid concentration (e.g. Figures 1f and 1l) were then compared with the gradient and r^2 values of the best-fit lines of the uncorrected f_e against lipid concentration.

Results:

In all experiments, the phase of both water and dioxane varied linearly with time throughout the samples as expected. Results of the primary analysis, not taking into account potential bias due to unexpected variations in dioxane concentration, are shown in Figure 1. Representative maps

of exchange-induced frequency shifts are shown in Figures 1a and 1g. In Figures 1b and 1h, the ROIs are shown overlaid on magnitude water images at TE = 9.57 ms, together with the cerebroside / POPC concentrations.

Representative graphs of the mean f_e measured in the different lipid samples plotted against the cerebroside or POPC concentration are shown in Figures 1c and 1i respectively. The results of repeated experiments are also shown in Table 3. Since the gradients of the best-fit lines did not change much over the repeated experiments, the best-fit line gradients and r^2 values were averaged over all GC and, separately, over all POPC experiments. The uncorrected exchange-induced frequency increased linearly with cerebroside concentration at 0.208 ± 0.027 ppb/mM ($r^2 = 0.936$, $p < 0.01$ in a two-sided t-test). This is in comparison with f_e at increasing concentrations of pure POPC which showed negligible increase with concentration at 0.018 ± 0.022 ppb/mM ($r^2 = 0.143$, $p > 0.45$ in a two-sided t-test). The results of fitting f_e against lipid concentration are summarized in Table 3.

Effects of Dioxane Concentration on Water Frequency Shift

The results of the water-dioxane experiments are presented in Figures 2 and 3. Figure 2a shows a map of $f_{w\text{-}d}$ and illustrates the fact that the shifts in this experiment were much greater than those measured in the lipid experiments. Figure 2b shows the measured peak area ratio (R) against 1/water molar fraction (wmf). R shows a strong linear dependence on wmf ($r^2 > 0.99$). However, the coefficients do not agree exactly with the assumption that R is directly proportional to the number of dioxane protons/number of water protons i.e. they are not equal to 4 as predicted in Equation 2. Figure 2c shows the measured frequency shift $f_{w\text{-}d}$ against the measured peak area ratio. This shows a strong linear relationship which was used for correction of the initial lipid results shown above.

To allow comparison with the previous results of Leutritz et al. (16), we also plotted $f_{w\text{-}d}$ against the dioxane concentration (Fig. 3). As Leutritz et al. (16) found a linear relationship between $f_{w\text{-}d}$ and the dioxane concentration we performed a linear fit over all of our data which gave a gradient of –0.0504 ± 0.0041 ppb/mM and $r^2 = 0.9626$. As our dioxane concentrations were far higher than those used in Leutritz et al (16) we also performed a linear fit over the four lowest dioxane concentrations for a closer comparison which gave an improved fit with a gradient of –0.0206 ± 0.0022 ppb/mM and $r^2 = 0.9782$. The data were fitted to the relationship given in (19) which yielded a much closer fit ($r^2 = 0.9984$) than the linear fits described above.

Correction for Unexpected Small Variations in Dioxane Concentrations in Lipid Experiments

Examples of the effect of correcting the measured lipid f_e values are shown in Figures 1f and 1l. Figures 1d and 1j show examples of peak area ratios measured in the lipid experiments. These were used together with the best-fit linear relationship between $f_{w\text{-}d}$ and R (Figure 2c) to calculate a predicted additional dioxane-induced frequency shift shown in Figures 1e and 1k for GC and POPC respectively. Note that the peak area ratios showed different behavior with increasing lipid concentration in the different lipid experiments (Figures 1d and 1j) and that the frequency shifts predicted from them were thus also different (Figures 1e and 1k). The results of subtracting the additional shifts over the baseline/intercept given in Figures 1e and 1k from the original f_e values in Figures 1c and 1i gave the corrected shifts shown in Figures 1f and 1l respectively.

The results of fitting the corrected f_e against lipid concentration are summarised in Table 3 together with the uncorrected results. The correction resulted in the significant increase in the uncorrected f_e with GC concentration being abolished (corrected $\Delta f_{GC} = 0.023 \pm 0.037$ ppb/mM, $r^2 = 0.085$, $p > 0.575$ in a two-sided t-test) and also gave a significant increase in f_e with

increasing POPC concentration (Δf_{POPC} = 0.044 ± 0.008 ppb/mM, r^2 = 0.877, $p < 0.01$ in a two-sided t-test) which had not been observed in the uncorrected case.

Discussion:

The measurements presented here suggest that the contribution of lipids to exchange-induced frequency shifts f_e in white matter is likely to be small. Although significant variation in f_e was observed in samples with differing amounts of cerebrosides (GC) (26) and phospholipids (POPC), two of the main lipids found in cell membranes, much of this variation may be attributable to the effect of the internal frequency reference (dioxane) on the water frequency shift. Accurate measurement of this effect ($f_{w\text{-}d}$) in dioxane-water samples, and correction for its contribution to f_e in lipid samples, rendered the previously significant dependence of f_e on GC concentration insignificant. Interestingly, after correction, a small but significant dependence of f_e on POPC concentration was seen. This is counter-intuitive as POPC has only one exchangeable OH proton and almost no MT effect (14), suggesting that it does not contribute substantially to chemical exchange processes.

The corrected POPC-induced frequency shift coefficient (0.044 ± 0.008 ppb/mM), together with literature WM-GM tissue phospholipid concentrations (~ 35-38 mM (7,8)) suggests that we might expect ~ 1-2 ppb exchange-induced WM-GM contrast due to POPC. This is considerably smaller than brain tissue measurements: WM-GM Δf_e = 6.3 to 13.5 ppb (4) and is also smaller than the 6-12 ppb susceptibility anisotropy observed in WM at 7T (27).

To compare the results obtained here with previous measurements in protein solutions, we need to take into account the molecular weights of these lipids (760 g/mol, Avanti) relative to proteins (BSA, ~67 kg/mol, (5)), which are likely to be related to the number of exchanging

protons on each molecule. Taking this into consideration, the measured Δf_{POPC} ~ 0.06 ppb / (g/L) is smaller than the f_e measured previously in BSA protein solutions ~ 0.16 ppb / (g/L) (5,6), although the latter may have been influenced by dioxane- (or TSP-) water interactions as well.

Limitations and Assumptions:

The results presented above need careful interpretation. Apart from the difficulty in measuring small shifts in resonance frequency, and the ample opportunity for confounding effects, our model systems are, by definition, a highly simplified approximation of the conditions found in white matter *in vivo*. One shortcoming is the relatively low temperature used here (room temperature) compared to temperatures encountered *in vivo*. Since chemical exchange rates tend to increase with temperature and lineshapes change (23), we would expect exchange-induced frequency shifts to be different *in vivo* at body temperature. It is possible that the PBS buffer did not perfectly control the pH of the samples, leading to a potential confound to the measurements of f_e at different lipid concentrations. Any lipid concentration-dependent pH variations are likely to be small as POPC-GC and POPC-Cholesterol MLVs (14) with over three to six times the total lipid concentration in our samples buffered with 10mM HEPES buffer at pH 7.4 (c.f. our PBS with 3.0 mM Sodium Phosphate and 1.1 mM Potassium Phosphate) showed pH values between 7 and 7.4.

In the water-dioxane experiment, the dependence of dioxane: water peak area ratio R on the reciprocal of the water molar fraction was found to be 3.21, somewhat below the value expected based on the molar ratio of their proton concentrations (i.e. 4). This could be for a number of reasons including the fact that spectral peak areas are influenced by factors other than the number of dioxane and water protons present e.g. saturation and relaxation effects (25). This should not affect the corrections for the effect of dioxane on water frequency shift, assuming this phenomenon was present similarly in the water-dioxane samples and in the lipid samples.

A noticeable feature of the best fit lines for the variation of exchange-induced frequency plotted against lipid concentration (e.g. in Figs. 1c and 1i) was a different constant offset in each experiment. These different offsets meant that the f_e measured in the 'control' tubes could not be compared between experiments and are, therefore, not shown. The different offsets are likely to arise from subtraction of the mean apparent f_e in the surrounding fluid ROI (large blue ROI in Figures 1b and 1h) from all the other mean ROI values in an attempt to correct for any slight mis-centering of the band-pass filters over the water and dioxane spectral peaks. Therefore, any offset is likely to depend greatly on the precise choice of fluid ROI, especially because the SD of f_e in the largest fluid ROI was much greater than within any of the lipid ROIs. Fortunately, the different offsets do not affect the findings regarding the observed dependencies of f_e on lipid concentrations as these are based only on the gradients and r^2 values of the best-fit lines.

Figure 3 clearly shows a strong dependence of $f_{w\text{-}d}$ on the concentration of dioxane in each sample. At the lowest concentrations the gradient of the best-fit line ($-2.06 \pm 0.22 \times 10^{-5}$ ppm/mM dioxane) agrees reasonably well with the dependence measured by Leutritz et al. (16) ($-2.68 \pm 0.42 \times 10^{-5}$ ppm/mM dioxane). We performed $f_{w\text{-}d}$ measurements at dioxane concentrations (534 - 6352 mM - Table 2) much greater than those of Leutritz et al. (0-60 mM). At these higher concentrations the relationship between $f_{w\text{-}d}$ and dioxane concentration becomes non-linear and behaves according to the relationship given in (19) (Fig. 3). This $f_{w\text{-}d}$ - [dioxane] relationship can be predicted by considering dioxane-water complex formation through hydrogen bonds as has been previously observed in (18,19). This non-linear relationship becomes linear again when $f_{w\text{-}d}$ is plotted against R instead of just the dioxane concentration (Figure 2c).

Despite the fact that the dioxane:water concentration was designed to be constant throughout all the lipid tubes and the surrounding fluid (15% v/v giving a predicted peak area of 0.127), small variations in the measured peak area ratio (R) were found between the different lipid tubes e.g.

between 0.105 to 0.122 (see Figures 1d and 1j). It is not clear why R was variable and slightly less than expected (0.127). If anything, one might have expected a reduction in the water peak area, giving an increased R, due to the freeze-thawing during MLV formation or due to association of water with the lipids. Plots of R against lipid concentrations (Figures 1d and 1j) show that R decreased with increasing GC (and POPC) concentration in the GC experiments (Fig. 1d) and increased with POPC concentration in one of the POPC experiments (Fig. 1j) and showed no correlation with POPC concentration in the other (not shown). A potential explanation for these effects could be some sort of differential compartmentalisation of the dioxane and/or the water so that they reside in different proportions in the three available compartments: in between the lipid bilayers, inside the MLVs or outside them. If this differential compartmentalisation of dioxane and water were to explain the different behavior of R with lipid concentration for GC+POPC MLVs and pure POPC MLVs then the compartmentalisation would then also need to be different between these two types of MLVs.

The significant dependence of the corrected f_e on POPC concentration is intriguing considering POPC has only a single exchangeable OH proton per molecule. Given that the GC MLVs also contained POPC (GC:POPC 1:2), one might conclude that GC may have an opposing (and doubly large) effect on f_e compared to POPC. This would then suggest that the effects of GC and POPC on f_e result from exchangeable protons with different chemical shifts. This implies that the magnitude of f_e may vary considerably depending on the relative concentration of particular lipid species.

A further possibility is that, in addition to the measured interactions between dioxane and water, dioxane may also interact directly with lipids, making it an even less desirable reference substance. There is some evidence that dioxane could interact with lipids as it has been used as a solvent for lipids (28-30) and has been found to disrupt hydrophobic lipid-protein interactions (31). Furthermore, the dioxane resonance frequency has been found to shift in PBS when

compared with pure water (22). Future experiments to test whether lipid-dioxane interactions could have affected these results could involve replication of the water-dioxane experiment with multilamellar vesicles present at a constant lipid concentration. If the results were significantly different from those shown here in Figures 2 and 3 then this would provide evidence for the water-dioxane interaction being affected by the presence of lipids.

In order to completely eliminate the influence of interactions between the reference chemical and the water or lipids on the results of future experiments, it would be necessary to devise a reference-chemical-free method for measuring exchange-induced frequency shifts. This is difficult to do because the primary reason for using internal reference chemicals is to allow removal of the susceptibility-induced frequency shifts. This separation of exchange-induced and susceptibility-induced frequency shifts cannot be done using an external reference or while the magnetic susceptibilities of cerebrosides and POPC are still unknown.

If a reference-free method to measure f_e shifts can be developed, it might be interesting to investigate lipid-based f_e contrast in neurological diseases as phospholipids such as POPC are a primary constituent of cell membranes and cerebrosides are essential for axonal myelin membrane integrity (32-34).

Conclusion:

Exchange-induced frequency shifts f_e were measured in MLVs formed from cerebrosides (GC) and phospholipids (POPC) developed here to model WM cell membranes. Based on a confounding effect due to unexpected small variations in the concentration of dioxane, which was used as an internal frequency reference to remove susceptibility-induced frequency shifts, we devised a method to correct the MLV data. Following this correction, a significant increase in uncorrected f_e with GC concentration was abolished and a small but significant linear increase in f_e with POPC concentration was observed: $\Delta f_{POPC} = 0.044 \pm 0.008$ ppb/mM. Straightforward

interpretation would suggest that lipids add no more than a minor contribution to f_e and, more generally, to frequency variations observed in brain tissue. However, generalizing these findings to the *in-vivo* case should be done tentatively, partly because of the difficulty in realistic modelling of the conditions encountered *in vivo* and partly because of the limitations of the method used to correct the MLV data. In addition, further research is needed to develop a reference-chemical-free method that can separate exchange-induced from susceptibility-induced frequency shifts so that the specific contributions from individual lipids can be more accurately quantified.

Acknowledgements:

We thank Dr Eugenia Poliakov and Dr Christian Wunder for extensive help with vesicle preparation and Dr Peter Macdonald for useful advice and discussions. We are grateful to Dr Doug Morris for practical assistance with chemical shift imaging experiments and useful discussions and to Stephanie French for laboratory support. We thank Dr Jacco de Zwart for computer and programming support. This research was supported by the intramural research program of the National Institute for Neurological Disorders and Stroke at the National Institutes of Health.

References:

1. Duyn JH, van Gelderen P, Li TQ, de Zwart JA, Koretsky AP, Fukunaga M. High-field MRI of brain cortical substructure based on signal phase. *Proc Natl Acad Sci U S A* 2007;104(28):11796-11801.

2. Shmueli K, de Zwart JA, van Gelderen P, Li TQ, Dodd SJ, Duyn JH. Magnetic susceptibility mapping of brain tissue in vivo using MRI phase data. *Magn Reson Med* 2009;62(6):1510-1522.

3. Mark Haacke E, Reichenbach JR, Wang Y. Susceptibility-Weighted Imaging and Quantitative Susceptibility Mapping. *Brain Mapping: An Encyclopedic Reference*. Volume 1; 2015. p 161-172.

4. Shmueli K, Dodd SJ, Li TQ, Duyn JH. The contribution of chemical exchange to MRI frequency shifts in brain tissue. *Magn Reson Med* 2011;65(1):35-43.

5. Luo J, He X, d'Avignon DA, Ackerman JJ, Yablonskiy DA. Protein-induced water 1H MR frequency shifts: contributions from magnetic susceptibility and exchange effects. *J Magn Reson* 2010;202(1):102-108.

6. Zhong K, Leupold J, von Elverfeldt D, Speck O. The molecular basis for gray and white matter contrast in phase imaging. *Neuroimage* 2008;40(4):1561-1566.

7. Norton WT, Cammer W. Isolation and Characterization of Myelin. In: Morell P, editor. *Myelin*. 2nd ed. New York: Plenum Press; 1984. p 155.

8. O'Brien JS, Sampson EL. Lipid composition of the normal human brain: gray matter, white matter, and myelin. *J Lipid Res* 1965;6(4):537-544.

9. Wennekes T, van den Berg RJ, Boot RG, van der Marel GA, Overkleeft HS, Aerts JM. Glycosphingolipids--nature, function, and pharmacological modulation. *Angew Chem Int Ed Engl* 2009;48(47):8848-8869.

10. Tan RX, Chen JH. The cerebrosides. *Nat Prod Rep* 2003;20(5):509-534.

11. Wiegandt H, editor. Glycolipids. Volume 10. Amsterdam: Elsevier; 1985.

12. Zaraiskaya T, Jeffrey KR. Molecular dynamics simulations and 2H NMR study of the GalCer/DPPG lipid bilayer. *Biophys J* 2005;88(6):4017-4031.

13. Fidorra M, Heimburg T, Bagatolli LA. Direct visualization of the lateral structure of porcine brain cerebrosides/POPC mixtures in presence and absence of cholesterol. *Biophys J* 2009;97(1):142-154.

14. Kucharczyk W, Macdonald PM, Stanisz GJ, Henkelman RM. Relaxivity and magnetization transfer of white matter lipids at MR imaging: importance of cerebrosides and pH. *Radiology* 1994;192(2):521-529.

15. Skarjune R, Oldfield E. Physical studies of cell surface and cell membrane structure. Deuterium nuclear magnetic resonance studies of N-palmitoylglucosylceramide (cerebroside) head group structure. *Biochemistry* 1982;21(13):3154-3160.

16. Leutritz T, Hilfert L, Smalla KH, Speck O, Zhong K. Accurate quantification of water-macromolecule exchange induced frequency shift: Effects of reference substance. *Magnetic Resonance in Medicine* 2013;69(1):263-268.

17. Leutritz T, Hilfert L, Smalla K-H, Speck O, Zhong K. Accurate Determination of Water-Macromolecule Exchange Independent of Reference Interaction. *Proc Intl Soc Mag Reson Med* 2011;19:4526.

18. Mizuno K, Imafuji S, Fujiwara T, Ohta T, Tamiya Y. Hydration of the CH groups in 1,4-dioxane probed by NMR and IR: Contribution of blue-shifting CH center dot center dot center dot OH2 hydrogen bonds. *J Phys Chem B* 2003;107(16):3972-3978.

19. Fratiello A, Douglass DC. NMR shift and diffusion study of dioxane-H2O and pyridine-H2O mixtures. *Journal of Molecular Spectroscopy* 1963;11(1):465-482.

20. Hope MJ, Bally MB, Mayer LD, Janoff AS, Cullis PR. Generation of Multilamellar and Unilamellar Phospholipid-Vesicles. *Chemistry and Physics of Lipids* 1986;40(2-4):89-107.

21. Shimizu A, Ikeguchi M, Sugai S. Appropriateness of Dss and Tsp as Internal References for H-1-Nmr Studies of Molten Globule Proteins in Aqueous-Media. *Journal of Biomolecular Nmr* 1994;4(6):859-862.

22. Luo J, He X, Yablonskiy DA. Magnetic susceptibility induced white matter MR signal frequency shifts - Experimental comparison between Lorentzian sphere and generalized Lorentzian approaches. *Magnetic Resonance in Medicine* 2014;71(3):1251-1263.

23. Levitt MH. *Spin Dynamics. Basics of Nuclear Magnetic Resonance*. Chichester, England: John Wiley & Sons Ltd; 2008. p 493-496.

24. Conturo TE, Smith GD. Signal-to-noise in phase angle reconstruction: dynamic range extension using phase reference offsets. *Magn Reson Med* 1990;15(3):420-437.

25. Drost DJ, Riddle WR, Clarke GD. Proton magnetic resonance spectroscopy in the brain: report of AAPM MR task group #9. *Medical Physics* 2002;29(9):2177-2197.

26. Shmueli K, Dodd SJ, Wunder C, Duyn J. Could Lipids Contribute to the Exchange-Induced Resonance Frequency Contrast in Brain Tissue? *Proceedings 20th Scientific Meeting, International Society for Magnetic Resonance in Medicine* 2011;19:704.

27. Lee J, Shmueli K, Fukunaga M, van Gelderen P, Merkle H, Silva AC, Duyn JH. Sensitivity of MRI resonance frequency to the orientation of brain tissue microstructure. *Proc Natl Acad Sci U S A* 2010;107(11):5130-5135.

28. Mukhopadhyay L, Bhattacharya PK, Moulik SP. Thermodynamics of water-induced precipitation of cholesterol and its acetate, benzoate and stearate derivatives dissolved in 1,4-dioxane and 2-propanol. *Indian J Biochem Biophys* 1989;26(5):340-342.

29. Mukhopadhyay L, Ray J, Das S, Bhattacharya PK, Moulik SP. Water-induced precipitation of cholesterol dissolved in organic solvents in the absence and presence of surfactants and salts. *Indian J Biochem Biophys* 1989;26(3):178-185.

30. Forti FL, Goissis G, Plepis AMG. Modifications on collagen structures promoted by 1,4-dioxane improve thermal and biological properties of bovine pericardium as a biomaterial. *J Biomater Appl* 2006;20(3):267-285.

31. Dees C, German TL, Wade WF, Marsh RF. Characterization of lipids in membrane vesicles from scrapie-infected hamster brain. *Journal of General Virology* 1985;66(4):861-870.

32. Boggs JM, Gao W, Hirahara Y. Myelin glycosphingolipids, galactosylceramide and sulfatide, participate in carbohydrate-carbohydrate interactions between apposed membranes and may form glycosynapses between oligodendrocyte and/or myelin membranes. *Biochim Biophys Acta* 2008;1780(3):445-455.

33. Boggs JM, Gao W, Zhao J, Park HJ, Liu Y, Basu A. Participation of galactosylceramide and sulfatide in glycosynapses between oligodendrocyte or myelin membranes. *FEBS Lett* 2010;584(9):1771-1778.

34. Bosio A, Binczek E, Stoffel W. Functional breakdown of the lipid bilayer of the myelin membrane in central and peripheral nervous system by disrupted galactocerebroside synthesis. *Proc Natl Acad Sci U S A* 1996;93(23):13280-13285.

Table 1: Concentrations of Lipids (mM) in MLV Samples with Molar Fractions (%) of all Components

Note that the final lipid concentrations (mM) in each tube after the addition of 15% v/v dioxane were equal to the values in the first three columns of the table divided by 1.15.

Concentration (mM)				Molar Fraction (%)		
Cerebrosides	POPC	Total Lipids	ROI Color	Total Lipids	Water	Dioxane
4	8	12	green	0.021	96.900	3.079
11	22	33	yellow	0.058	96.864	3.078
18	36	54	pink	0.094	96.829	3.077
25	50	75	cyan	0.131	96.793	3.076
32	64	96	orange	0.168	96.758	3.075
39	78	117	purple	0.204	96.722	3.074

Table 2: Concentrations of Water and Dioxane in the Water-Dioxane Experiment

The large outer tube was included as a data point in this experiment and contained the lowest dioxane concentration. Note that the concentration of water and dioxane in the lipid MLV experiments was nominally closest to the highlighted row in the table i.e. 15% v/v dioxane/water corresponds to a water concentration of 48,169 mM and a dioxane concentration of 1,531 mM.

Molar fraction of water	Molar fraction of Dioxane	Water concentration (mM)	Dioxane concentration (mM)
0.99	0.01	52873	534
0.98	0.02	50527	1031
0.97	0.03	48337	1495
0.96	0.04	46290	1929
0.93	0.07	40873	3076
0.90	0.10	36337	4037
0.85	0.15	30221	5333
0.80	0.20	25409	6352

Table 3: Summary of the Results of Experiments to Measure f_e in Lipid MLVs

Gradients of best-fit lines (with standard errors) for both uncorrected and corrected exchange-induced frequency shifts f_e against lipid concentration. r^2 values are also shown for the best fit lines together with p values for the mean r^2 values from a two-sided t-test.

						Corrected for Water-Dioxane Frequency Shift			
Experiment	**Repetition**	**Gradient of fe v. lipid concentration (ppb/mM)**	**SE on gradient of fe v. lipid concentration (ppb/mM)**	**r^2**	**p**	**Gradient of fe v. lipid concentration (ppb/mM)**	**SE on gradient of fe v. lipid concentration (ppb/mM)**	**r^2**	**p**
GC	1	0.208	0.027	0.937		0.023	0.046	0.058	
	2	0.208	0.027	0.935		0.023	0.032	0.111	
	Mean	**0.208**	**0.027**	**0.936**	**0.002**	**0.023**	**0.037**	**0.085**	**0.576**
POPC 1	1	0.043	0.025	0.421		0.045	0.006	0.930	
POPC 2	1	0.006	0.018	0.025		0.043	0.009	0.844	
	2	0.011	0.021	0.067		0.045	0.009	0.866	
	3	0.010	0.020	0.059		0.043	0.008	0.869	
	Mean	**0.018**	**0.022**	**0.143**	**0.460**	**0.044**	**0.008**	**0.877**	**0.006**

FIGURE LEGENDS

Figure 1. Results of Measuring f_e in Lipid Experiments

Exchange-induced frequency maps in the GC (a) and POPC (g) experiments. The exchange-induced frequency maps are scaled between -2 and +3 Hz. The magnitude images at TE = 9.6 ms are shown in figures (b) and (h) together with ROIs used to obtain the mean and standard deviation of f_e in each tube. The lipid concentrations in each tube increase from green (A lowest concentration) to yellow, pink, cyan, orange, and purple (F highest concentration) (see Table 1). The large blue ROI indicates the surrounding PBS and the black circles are air bubbles that were excluded from the ROI analysis. The graphs in (c) and (i) show the mean exchange-induced frequency in each ROI plotted against the cerebroside (c) or POPC (i) concentration in each tube. The graphs in (f) and (l) show the corrected f_e values plotted against the cerebroside (f) or POPC (l) concentration in each tube. The peak area ratios (R) measured in the GC (d) and POPC (j) experiments are plotted against the relevant lipid concentration in each tube; the value from the surrounding PBS has been added as the '0 mM' value. These values, together with the linear relationship from the best-fit of $f_{w\text{-}d}$ v. R (Figure 2c) were used to calculate a predicted additional frequency shift shown in (e) and (k) for GC and POPC respectively. The corrected values in (f) and (l) were obtained by subtracting the additional frequency shift (i.e. the frequency shift minus the intercept of the best-fit line) in (e) and (k) from the original frequency shifts in (c) and (i) respectively. In figures (c-f) and (i-l) the best-fit lines are given, together with the r^2 values. The error bars on each point indicate the standard deviation in each ROI.

Figure 2. Results of Measuring $f_{w\text{-}d}$ in Water-Dioxane Experiments

Exchange-induced frequency $f_{w\text{-}d}$ map for the different water/dioxane concentrations shown in Table 2 (a) scaled between -139 and+ 91 Hz. Peak area ratio R (dioxane:water) plotted against the inverse of the water molar fraction for the water/dioxane mixtures at different concentrations to test the predicted relationship in Equation 2 (b). The best-fit line is shown together with the r^2 value. The measured interaction-induced water-dioxane frequency shift $f_{w\text{-}d}$ for the

water/dioxane mixtures at different concentrations plotted against the measured peak area ratio R (dioxane:water) (c). The best-fit line is shown together with the r^2 value and this relationship was used together with the measured peak area ratios in each lipid tube to correct the measured f_e values in the lipid experiments. The error bars on each point in the graphs indicate the standard deviation in each ROI. Note that the total frequency difference between dioxane and water peaks would be given by the interaction-induced shift $f_{w\text{-}d}$ plotted here in addition to the expected chemical shift difference between dioxane and water (1.04 ppm) (4) and thus remains positive over the whole range of peak area ratios.

Figure 3. Results of Measuring $f_{w\text{-}d}$ v. Dioxane Concentration in Water-Dioxane Experiments

Exchange-induced frequency $f_{w\text{-}d}$ plotted against dioxane concentration (black ×s). For comparison with Leutritz et al. (16), a linear fit was performed over the four lowest dioxane concentrations giving a gradient of -0.0206 ± 0.0022 ppb/mM and $r^2 = 0.9782$. The relationship given in (19) is shown to fit the data closely: $r^2 = 0.9984$. The error bars on each point in the graphs indicate the standard deviation in each ROI therefore the point at the lowest concentration has the largest error because it came from the largest (outer tube) ROI. Note that the total frequency difference between dioxane and water peaks would be given by the interaction-induced shift $f_{w\text{-}d}$ in addition to the expected chemical shift difference between dioxane and water (1.04 ppm) (4) and thus remains positive over the whole concentration range.

Investigating Lipids as a Source of Chemical Exchange-Induced MRI Frequency Shifts

K. Shmueli[1,2], S. J. Dodd[3], P. van Gelderen[1] and J. H. Duyn[1]

1. Advanced MRI Section, Laboratory of Functional & Molecular Imaging, National Institute of Neurological Disorders & Stroke, National Institutes of Health, USA
2. Department of Medical Physics & Biomedical Engineering, University College London, UK
3. Laboratory of Functional & Molecular Imaging, National Institute of Neurological Disorders & Stroke, National Institutes of Health, USA

Word Count

5,312 words

Sponsors

This research was supported by the intramural research program of the National Institute for Neurological Disorders and Stroke at the National Institutes of Health.

Karin Shmueli is partly supported by the Engineering and Physical Research Council grant EP/K027476/1.

Keywords

Chemical Exchange

Exchange-Induced Resonance Frequency Shifts

Chemical shift imaging

Dioxane

Multilamellar Lipid Vesicles

Phospholipids

Abbreviations:

BSA	bovine serum albumin
CSI	chemical shift MR imaging
d	dioxane concentration
dmf	dioxane molar fraction
f_e	Exchange-induced frequency shift
$f_{w\text{-}d}$.	Additional interaction-induced water frequency shift relative to dioxane frequency shift
GalCer	galactosylceramides
GC	Galactocerebroside
GM	gray matter
MLVs	multilamellar vesicles
MT	magnetization transfer
NH	amide
OH	hydroxyl
PBS	phosphate-buffered saline
POPC	phospholipid: 16:0-18:1 PC, 1-palmitoyl-2-oleoyl-*sn*-glycero-3-phosphocholine
R	peak area ratio (dioxane:water) should be proportional to the relative concentration of dioxane to water
ROI	region of interest
SNR	signal-to-noise ratio
TSP	3-(trimethylsilyl)-propionic acid-d_4 sodium salt, also called Sodium 3-(trimethylsilyl)-propionate-2,2,3,3-d_4 or 2,2,3,3,-tetradeutero-3-trimethylsilylpropionic acid
w	water concentration
WM	white matter
wmf	water molar fraction

Abstract:

While magnetic susceptibility is a major contributor to NMR resonance frequency variations in human brain, a substantial contribution may come from chemical exchange of protons between water and other molecules. Exchange-induced frequency shifts f_e have been measured in tissue and protein solutions but relatively lipid-rich white matter (WM) has a larger f_e than gray matter, suggesting that lipids could contribute. Galactocerebrosides (GC) are a prime candidate as they are abundant in WM and susceptible to exchange. To investigate this, f_e was measured in a model of WM lipid membranes in the form of multilamellar vesicles (MLVs), consisting of a 1:2 molar ratio of GC and phospholipids (POPC), and in MLVs with POPC only. Chemical shift imaging with 15% volume fraction of dioxane, an internal reference whose protons are assumed not to undergo chemical exchange, was used to remove susceptibility-induced frequency shifts in an attempt to measure f_e in MLVs at several lipid concentrations. Initial analysis of these measurements indicated a necessity to correct for small unexpected variations in dioxane concentration due to its effect on the water frequency shift. To achieve this, actual dioxane concentration was inferred from spectral analysis and its additional contribution to f_e was removed through separate experiments which showed that the water-dioxane frequency shift depended linearly on the dioxane concentration at low concentrations with a proportionality constant of –0.021 ± 0.002 ppb/mM in agreement with published experiments. Contrary to expectations and uncorrected results, for GC+POPC vesicles, the dependence of the corrected f_e on GC concentration was insignificant (0.023 ± 0.037 ppb/mM; $r^2 = 0.085$, $p>0.57$), while for the POPC-only vesicles a small but significant linear increase with POPC concentration was found: 0.044 ± 0.008 ppb/mM ($r^2 = 0.877$, $p<0.01$). These findings suggest that the non-susceptibility contribution of lipids to frequency contrast in WM may be small.

Introduction:

Gradient-echo MR frequency images are increasingly utilized because they provide high contrast that is complementary to conventional magnitude image contrast. Magnetic susceptibility is widely accepted as a major source of this tissue frequency contrast (1-3). In addition, recent measurements in fixed human and fresh pig brain tissues (4) show a substantial (and opposing) contribution to white-gray matter (WM-GM) frequency contrast from chemical exchange of protons between water and off-resonance molecular sites. Studies in protein solutions (5,6) also found a positive exchange-induced frequency shift (f_e) that was directly proportional to the concentration of bovine serum albumin (BSA) protein. On the basis of these protein studies, f_e contrast in brain tissue has been attributed to protons exchanging between water and protein amide (NH) and hydroxyl (OH) groups (6).

However, we cannot assume that proteins are the sole cause of the greater f_e observed in WM than in GM (4) given that both i) WM contains much less protein than GM (as a percentage of dry mass) (7) and ii) WM contains approximately 1.7 times the total lipid content of GM (as a percentage of dry mass) (7). The fact that the relatively lipid-rich WM has a larger f_e than GM suggests that there may be sites of exchange in lipids that contribute to the observed exchange-induced frequency shifts.

To begin to investigate whether lipids cause exchange-induced frequency shifts we chose to focus specifically on cerebrosides because they are a major component of human WM, constituting approximately 20% of the total lipid weight (7,8). Even more relevant for a potential cause of WM-GM f_e contrast, cerebrosides show the largest WM-GM difference of all the lipids, and are over three times more abundant in human WM than GM (7,8). Cerebrosides are ceramide-based glycosphingolipids (9-11) whose head groups consist of a single hexose sugar residue, with galactosylceramides (GalCer) or galactocerebrosides (GC) being most common in the central nervous system (12,13). Another reason why cerebrosides are a good

candidate for chemical exchange is that their head groups have several OH groups exposed at the surface of phospholipid cell membranes (14,15). These lipids have also been shown to cause large magnetization transfer (MT) effects that have been attributed to chemical exchange based on their pH-dependence (14).

Therefore, we tested the hypothesis that cerebrosides cause f_e, using an *in-vitro* model for WM cell membranes to investigate whether cerebrosides could contribute to the WM-GM f_e contrast in brain tissue.

Our chosen reference substance, dioxane, is known to affect the water frequency shift (16-19). Therefore, we kept the concentration of dioxane constant throughout our lipid experiments. We also set out to measure any dioxane-induced water frequency shifts separately in water/dioxane mixtures in the same experimental setup and incorporated any observed effects into our analysis of the lipid experiments.

Methods:

Choice of Lipids

To measure any f_e due to cerebrosides, a single-slice chemical shift MR imaging (CSI) experiment was performed in multi-lamellar vesicle samples containing several different concentrations of cerebrosides (GC). Multi-lamellar vesicles (MLV) are an authentic model for white matter; their onion-like structure closely resembles the multiple lipid bilayers of the myelin sheath on electron microscopy (20). However, because pure cerebrosides are highly insoluble in water and have a very high melting (gel to liquid crystalline) phase transition temperature (12,13) compared to other membrane lipids, they do not form stable multi-lamellar vesicles in aqueous solvents. For this reason, a phospholipid (16:0-18:1 PC, 1-palmitoyl-2-oleoyl-*sn*-glycero-3-phosphocholine, POPC), which is equivalent to naturally occurring

phosphatidylcholine, was included in all the lipid samples. A constant 2:1 POPC:GC molar ratio was chosen to approximate the phospholipid to glycolipid ratio in human WM (7,8,14).

To investigate whether cerebrosides led to exchange-induced frequency shifts, MLVs were made containing a range of cerebroside concentrations similar to those found in human WM. To test whether any observed exchange-induced frequency was caused by POPC, a control experiment was carried out using an identical setup but substituting pure POPC for cerebrosides to match the total lipid concentrations in each of the MLV samples.

Choice of Reference Chemical:

As in previous experiments (4,5), 1,4 dioxane was used as a reference chemical whose protons are assumed not to exchange with macromolecules. Dioxane was chosen over TSP (3-(trimethylsilyl)-propionic acid-d_4 sodium salt, also called Sodium 3-(trimethylsilyl)-propionate-2,2,3,3-d_4 or 2,2,3,3,-tetradeutero-3-trimethylsilylpropionic acid), which has also been used as a reference chemical in exchange experiments (4,6), because TSP has been found to interact slightly with macromolecules and has a chemical shift that varies with pH (21) suggesting that its protons do undergo chemical exchange with macromolecules (16). Dioxane, on the other hand, has been used as a reference in protein (5) and tissue experiments (4,22) and has been reported as an appropriate reference for proteins (21).

Prior to scanning, dioxane was added to all the lipid MLV samples as well as the surrounding phosphate-buffered saline (PBS) (see Fig. 1). Because local susceptibility-induced frequency shifts in a given voxel are identical for both water and dioxane protons, f_e can be measured by subtracting the dioxane frequency from the water frequency in every voxel; see Shmueli et al. (4) for theory. This relies on a key assumption that the frequency shift of the dioxane reference proton signal is only affected by susceptibility differences. Because recent work has highlighted that the frequency of water is affected by the dioxane concentration (16), we took care to keep

the dioxane concentration constant in all the MLV samples and the surrounding PBS. This was achieved by adding dioxane to all the samples at 15% volume ratio (i.e. 15% volume dioxane:volume PBS) at the final stage just before MR imaging. This concentration (15% v/v) was chosen to be high enough to provide sufficient SNR for dioxane peak detection within each CSI voxel (c.f. Luo et. al. (5)) and much lower than in (4) in an attempt to reduce systematic errors due to any unforeseen interactions. Each MLV sample (that had been rehydrated with 0.5 ml PBS – see below) had 75 µl of dioxane added and was thoroughly mixed. 7.5 ml of dioxane was mixed with 50 ml of PBS to make the solution used to fill the large outer tube.

Ultimately, regions of interest were drawn on maps of the exchange-induced frequency shift to allow calculation of any effect of increasing the cerebroside or POPC concentration on the measured f_e.

Preparation of Lipid MLV samples:

Stock solutions of lipids (16:0-18:1 PC 760.08 g/mol and total porcine brain cerebrosides - predominant species: 812.25 g/mol, average: 781.95 g/mol, Avanti Polar Lipids Inc., AL, USA), in chloroform for POPC and 2:1 chloroform: methanol for the cerebrosides were combined to achieve the desired range of lipid concentrations and molar ratio (2:1 POPC:GC). Six concentrations (shown Table 1 and in Figures 1b and 1h) were chosen to cover the range found in human WM and GM (7,8). The solvents were removed by slow evaporation under a vacuum, leaving a thin film of lipid. To form multi-lamellar vesicles (MLVs), the lipid films were rehydrated in equal volumes (0.5 ml) of heated (~75°C) phosphate-buffered saline (PBS) with 5 freeze-thaw cycles as in Kucharczyk et al. (14). The high temperature was needed because of the high cerebroside melting (gel to liquid crystalline) phase transition temperature (~70-90°C) (12,13). Freezing was achieved by immersing the sample vials in liquid Nitrogen, and thawing

was accomplished by immersing the vials in a water bath at approximately 75°C for 5 minutes. In each cycle, all samples were thoroughly vortexed for 1 minute after thawing.

Once prepared, dioxane, 15% v/v, was added to each MLV sample as well as the surrounding PBS taking care to mix thoroughly. Each MLV sample was transferred into a 5-mm diameter NMR tube (Wilmad Labglass, NJ, USA) and these smaller tubes (six tubes and an MLV 'control' tube – see below) were mounted into two PVC tube-holders designed to align and space the tubes regularly within a larger 25 mm-diameter NMR tube. The large outer NMR tube was filled with PBS (+15% dioxane v/v) to a level higher than that of all the lipid samples. In the GC experiment, a tube was filled with POPC MLVs at a concentration of 54 mM. Similarly, in the POPC experiment, a tube was filled with GC MLVs at a concentration of 18 mM GC (i.e. 54 mM total lipid). These extra tubes were intended as 'controls' in an attempt to allow cross-referencing between the different experiments.

Chemical Shift MR Imaging (CSI):

Single-slice chemical shift MR imaging (CSI) was performed using a 600 MHz vertical bore spectrometer (Bruker, Biospin) fitted with a birdcage radiofrequency (RF) coil of 30 mm internal diameter. The acquisition frequency was centered on the water peak prior to and after manual shimming before scanning. The CSI slice had 202 x 202 x 300 μm voxels and a matrix size of 124 x 124. The acquisition had a 45° flip angle and a spectral width of 10 kHz (100 μs per point) with 1024 time points and a delay of 1.57 ms before acquisition (to accommodate the RF pulse duration and phase encode gradients). The repetition time was 1 s and the total acquisition time was 4 hours, 16 minutes and 16 s. The bandwidth of the slice-selective RF pulse was 6.6 kHz. All scans were performed at stable room temperature and after the lipid samples had equilibrated to room temperature. This is important because chemical exchange rates are strongly dependent on temperature therefore exchange-induced frequency shifts are

expected to be influenced by temperature (23). The temperature in the scanner bore, close to the sample, was recorded throughout the scans. Across all experiments, the temperature ranged between 290.10 and 291.77°K) and varied by less than 0.1°K (or 0.2°K for the repeated GC measurement) within each experiment.

Data acquisition was repeated after 25 and a half hours (for the experiment with different GC concentrations) (GC repetition 2) to check the stability of the MLVs and the reproducibility of the results. For this reason a second control (POPC) experiment (POPC 2) was also done with new MLV lipid samples and PBS and identical parameters to the first POPC (POPC 1) and GC experiments. This second POPC experiment (POPC 2, repetition 1), was repeated after 18 hours (POPC 2, repetition 2) (with a slightly different slice position and a different shim) and again after 23 hours (POPC 2, repetition 3) with TR increased from 1s to 2s, flip angle increased from 45° to 60° and gradient spoiler strength increased from 15% to 40% to increase SNR and rule out any contributions from unwanted coherences.

Water-Dioxane Experiment:

To allow for the potential correction of f_e for unintended small variations in dioxane concentration, we attempted to quantitatively assess the contribution from the previously reported relationship between the water frequency shift and the dioxane concentration (16-19). For this purpose, we performed an experiment similar to the MLV experiments described above by varying the relative concentrations of water and dioxane only (with no lipids).

The same NMR tube configuration and spacers were used but were filled only with water and dioxane at concentrations given in Table 2. These concentrations were chosen to cover the range expected in our lipid experiments as well as to reproduce the results in (16,18). CSI experiments were performed with identical acquisition parameters to those described above. The data were

also analysed exactly as described below but now assuming that any apparent frequency shifts $f_{w\text{-}d}$ were due to interactions between dioxane and water as described in (16-19).

Data Analysis

Primary analysis was geared towards estimating f_e from the spectral shift between water and dioxane peaks as a function of lipid concentration in the GC+POPC and POPC samples. Additional analysis was performed to estimate the precise dioxane concentration, in order to correct the primary results for small variations in the dioxane concentration that may have affected f_e. For this purpose, the water/dioxane experiment was analyzed for the dependence of the water frequency shift on the dioxane concentration inferred from the dioxane spectral intensity. The primary analysis closely followed that in Shmueli et al (4). The first 512 points (51.2 ms) of the raw, time domain data were selected for further analysis because most of the signal had decayed by the end of that time window. To select separate water and dioxane signals, the data were Fourier transformed into the frequency (spectral) domain and band-pass filters were placed around the water and dioxane peaks. The filters had a width of 550 Hz and cosine transition zones of widths 120 Hz. The central 64 points of the filtered spectra were Fourier transformed back into the time-domain and a 2-D spatial Fourier transform was performed to give separate water and dioxane magnitude and phase images over time.

In each voxel, the water-dioxane phase difference was fitted over time using least-squares linear regression to obtain f_e as the gradient of the linear fit divided by 2π. The fitting algorithm was designed to be effective in unwrapping the phase difference in each voxel over time. To ensure that the phase difference was fit only over time points and in voxels at which it had a sufficient signal-to-noise ratio (SNR), low-signal voxels in air bubbles and glass tube walls were excluded from the fit by thresholding the water magnitude image, and only time points having a water

magnitude SNR greater than 10 were included in the fit. This meant that the standard deviation of the noise in the phase image at each time point included in the fit was less than 0.1 radians because the noise in the phase image is equal to $1/SNR_{mag}$ (24).

The fit results were used to create maps of the exchange-induced frequency shift, f_e, for each experiment (see Figures 1a and 1g). Regions of interest (ROIs) were placed on these f_e maps to allow calculation of any effect of increasing the cerebroside or POPC concentration on the measured f_e. To calculate the mean and standard deviation of f_e for each lipid concentration, ROIs were drawn in the MLV-containing NMR tubes and surrounding fluid. The ROIs were drawn on the magnitude (water) image at TE = 9.57 ms, taking care to mask out air bubbles, glass tube walls and any other areas of low signal. The mean and standard error of f_e were recorded for each ROI. Any apparent f_e in the PBS ROI was subtracted from the raw f_e map to correct for any frequency shifts caused by inaccurate centering of the spectral band-pass filters on the resonance peaks in the CSI data. This step relied on the assumption that there is no exchange (and therefore zero f_e) in the PBS due to the absence of lipids or other off-resonance exchanging protons.

Correction of the primary analysis of lipid samples for small variations in dioxane concentration proceeded as follows. As the frequency shift between water and dioxane resonance ($f_{w\text{-}d}$) depends on the relative concentration of water and dioxane (16-19) we first estimated the relative dioxane/water concentration for each lipid concentration using their peak area ratio. The area under a resonance peak in a spectrum should be directly proportional to the number of protons resonating at that chemical shift and to the concentration of that chemical species (25). Therefore, the peak area ratio (R) should be proportional to the relative concentration of dioxane and water. Because there are 8 protons per dioxane molecule and 2 per water molecule, the relative concentration of dioxane (d) to water (w)

$$d/w = R/4 \qquad [1]$$

Therefore

$$R = 4(1/wmf - 1) \quad [2]$$

where wmf is the water molar fraction = w /(w+d).

In all experiments, the peak area ratio was measured by integrating the amplitudes (25) of the central 64 points of the filtered water and dioxane spectra in each voxel and taking the ratio of these peak areas. All further calculations were based on the mean peak area ratios inside each of the ROIs defined as described above.

The measured frequency shifts in the water-dioxane experiment $f_{w\text{-}d}$ were found to vary linearly with the measured peak area ratio (see Fig. 2c). Therefore, this best-fit linear relationship between $f_{w\text{-}d}$ and the peak area ratio from the water-dioxane experiments was used to predict an expected water-dioxane frequency shift $f_{wd\text{-}pred}$ (e.g. Figures 1e and 1k) from the measured peak area ratio for each ROI in the lipid experiments (e.g. Figures 1d and 1j). Finally, the residual $f_{wd\text{-}pred}$ values – relative to the intercept of the best-fit line of $f_{wd\text{-}pred}$ against lipid concentration (e.g. Figures 1e and 1k) – were subtracted from the original lipid f_e values in the same ROI (e.g. Figures 1c and 1i) to obtain the corrected lipid f_e values (Figures 1f and 1l).. The gradient and r^2 values of the best-fit lines to these corrected f_e values against lipid concentration (e.g. Figures 1f and 1l) were then compared with the gradient and r^2 values of the best-fit lines of the uncorrected f_e against lipid concentration.

Results:

In all experiments, the phase of both water and dioxane varied linearly with time throughout the samples as expected. Results of the primary analysis, not taking into account potential bias due to unexpected variations in dioxane concentration, are shown in Figure 1. Representative maps

of exchange-induced frequency shifts are shown in Figures 1a and 1g. In Figures 1b and 1h, the ROIs are shown overlaid on magnitude water images at TE = 9.57 ms, together with the cerebroside / POPC concentrations.

Representative graphs of the mean f_e measured in the different lipid samples plotted against the cerebroside or POPC concentration are shown in Figures 1c and 1i respectively. The results of repeated experiments are also shown in Table 3. Since the gradients of the best-fit lines did not change much over the repeated experiments, the best-fit line gradients and r^2 values were averaged over all GC and, separately, over all POPC experiments. The uncorrected exchange-induced frequency increased linearly with cerebroside concentration at 0.208 ± 0.027 ppb/mM ($r^2 = 0.936$, $p < 0.01$ in a two-sided t-test). This is in comparison with f_e at increasing concentrations of pure POPC which showed negligible increase with concentration at 0.018 ± 0.022 ppb/mM ($r^2 = 0.143$, $p > 0.45$ in a two-sided t-test). The results of fitting f_e against lipid concentration are summarized in Table 3.

Effects of Dioxane Concentration on Water Frequency Shift

The results of the water-dioxane experiments are presented in Figures 2 and 3. Figure 2a shows a map of $f_{w\text{-}d}$ and illustrates the fact that the shifts in this experiment were much greater than those measured in the lipid experiments. Figure 2b shows the measured peak area ratio (R) against 1/water molar fraction (wmf). R shows a strong linear dependence on wmf ($r^2 > 0.99$). However, the coefficients do not agree exactly with the assumption that R is directly proportional to the number of dioxane protons/number of water protons i.e. they are not equal to 4 as predicted in Equation 2. Figure 2c shows the measured frequency shift $f_{w\text{-}d}$ against the measured peak area ratio. This shows a strong linear relationship which was used for correction of the initial lipid results shown above.

To allow comparison with the previous results of Leutritz et al. (16), we also plotted $f_{w\text{-}d}$ against the dioxane concentration (Fig. 3). As Leutritz et al. (16) found a linear relationship between $f_{w\text{-}d}$ and the dioxane concentration we performed a linear fit over all of our data which gave a gradient of –0.0504 ± 0.0041 ppb/mM and $r^2 = 0.9626$. As our dioxane concentrations were far higher than those used in Leutritz et al (16) we also performed a linear fit over the four lowest dioxane concentrations for a closer comparison which gave an improved fit with a gradient of –0.0206 ± 0.0022 ppb/mM and $r^2 = 0.9782$. The data were fitted to the relationship given in (19) which yielded a much closer fit ($r^2 = 0.9984$) than the linear fits described above.

Correction for Unexpected Small Variations in Dioxane Concentrations in Lipid Experiments

Examples of the effect of correcting the measured lipid f_e values are shown in Figures 1f and 1l. Figures 1d and 1j show examples of peak area ratios measured in the lipid experiments. These were used together with the best-fit linear relationship between $f_{w\text{-}d}$ and R (Figure 2c) to calculate a predicted additional dioxane-induced frequency shift shown in Figures 1e and 1k for GC and POPC respectively. Note that the peak area ratios showed different behavior with increasing lipid concentration in the different lipid experiments (Figures 1d and 1j) and that the frequency shifts predicted from them were thus also different (Figures 1e and 1k). The results of subtracting the additional shifts over the baseline/intercept given in Figures 1e and 1k from the original f_e values in Figures 1c and 1i gave the corrected shifts shown in Figures 1f and 1l respectively.

The results of fitting the corrected f_e against lipid concentration are summarised in Table 3 together with the uncorrected results. The correction resulted in the significant increase in the uncorrected f_e with GC concentration being abolished (corrected $\Delta f_{GC} = 0.023 \pm 0.037$ ppb/mM, $r^2 = 0.085$, $p > 0.575$ in a two-sided t-test) and also gave a significant increase in f_e with

increasing POPC concentration (Δf_{POPC} = 0.044 ± 0.008 ppb/mM, r^2 = 0.877, $p < 0.01$ in a two-sided t-test) which had not been observed in the uncorrected case.

Discussion:

The measurements presented here suggest that the contribution of lipids to exchange-induced frequency shifts f_e in white matter is likely to be small. Although significant variation in f_e was observed in samples with differing amounts of cerebrosides (GC) (26) and phospholipids (POPC), two of the main lipids found in cell membranes, much of this variation may be attributable to the effect of the internal frequency reference (dioxane) on the water frequency shift. Accurate measurement of this effect ($f_{w\text{-}d}$) in dioxane-water samples, and correction for its contribution to f_e in lipid samples, rendered the previously significant dependence of f_e on GC concentration insignificant. Interestingly, after correction, a small but significant dependence of f_e on POPC concentration was seen. This is counter-intuitive as POPC has only one exchangeable OH proton and almost no MT effect (14), suggesting that it does not contribute substantially to chemical exchange processes.

The corrected POPC-induced frequency shift coefficient (0.044 ± 0.008 ppb/mM), together with literature WM-GM tissue phospholipid concentrations (~ 35-38 mM (7,8)) suggests that we might expect ~ 1-2 ppb exchange-induced WM-GM contrast due to POPC. This is considerably smaller than brain tissue measurements: WM-GM Δf_e = 6.3 to 13.5 ppb (4) and is also smaller than the 6-12 ppb susceptibility anisotropy observed in WM at 7T (27).

To compare the results obtained here with previous measurements in protein solutions, we need to take into account the molecular weights of these lipids (760 g/mol, Avanti) relative to proteins (BSA, ~67 kg/mol, (5)), which are likely to be related to the number of exchanging

protons on each molecule. Taking this into consideration, the measured $\Delta f_{POPC} \sim 0.06$ ppb / (g/L) is smaller than the f_e measured previously in BSA protein solutions ~ 0.16 ppb / (g/L) (5,6), although the latter may have been influenced by dioxane- (or TSP-) water interactions as well.

Limitations and Assumptions:

The results presented above need careful interpretation. Apart from the difficulty in measuring small shifts in resonance frequency, and the ample opportunity for confounding effects, our model systems are, by definition, a highly simplified approximation of the conditions found in white matter *in vivo*. One shortcoming is the relatively low temperature used here (room temperature) compared to temperatures encountered *in vivo*. Since chemical exchange rates tend to increase with temperature and lineshapes change (23), we would expect exchange-induced frequency shifts to be different *in vivo* at body temperature. It is possible that the PBS buffer did not perfectly control the pH of the samples, leading to a potential confound to the measurements of f_e at different lipid concentrations. Any lipid concentration-dependent pH variations are likely to be small as POPC-GC and POPC-Cholesterol MLVs (14) with over three to six times the total lipid concentration in our samples buffered with 10mM HEPES buffer at pH 7.4 (c.f. our PBS with 3.0 mM Sodium Phosphate and 1.1 mM Potassium Phosphate) showed pH values between 7 and 7.4.

In the water-dioxane experiment, the dependence of dioxane: water peak area ratio R on the reciprocal of the water molar fraction was found to be 3.21, somewhat below the value expected based on the molar ratio of their proton concentrations (i.e. 4). This could be for a number of reasons including the fact that spectral peak areas are influenced by factors other than the number of dioxane and water protons present e.g. saturation and relaxation effects (25). This should not affect the corrections for the effect of dioxane on water frequency shift, assuming this phenomenon was present similarly in the water-dioxane samples and in the lipid samples.

A noticeable feature of the best fit lines for the variation of exchange-induced frequency plotted against lipid concentration (e.g. in Figs. 1c and 1i) was a different constant offset in each experiment. These different offsets meant that the f_e measured in the 'control' tubes could not be compared between experiments and are, therefore, not shown. The different offsets are likely to arise from subtraction of the mean apparent f_e in the surrounding fluid ROI (large blue ROI in Figures 1b and 1h) from all the other mean ROI values in an attempt to correct for any slight mis-centering of the band-pass filters over the water and dioxane spectral peaks. Therefore, any offset is likely to depend greatly on the precise choice of fluid ROI, especially because the SD of f_e in the largest fluid ROI was much greater than within any of the lipid ROIs. Fortunately, the different offsets do not affect the findings regarding the observed dependencies of f_e on lipid concentrations as these are based only on the gradients and r^2 values of the best-fit lines.

Figure 3 clearly shows a strong dependence of $f_{w\text{-}d}$ on the concentration of dioxane in each sample. At the lowest concentrations the gradient of the best-fit line ($-2.06 \pm 0.22 \times 10^{-5}$ ppm/mM dioxane) agrees reasonably well with the dependence measured by Leutritz et al. (16) ($-2.68 \pm 0.42 \times 10^{-5}$ ppm/mM dioxane). We performed $f_{w\text{-}d}$ measurements at dioxane concentrations (534 - 6352 mM - Table 2) much greater than those of Leutritz et al. (0-60 mM). At these higher concentrations the relationship between $f_{w\text{-}d}$ and dioxane concentration becomes non-linear and behaves according to the relationship given in (19) (Fig. 3). This $f_{w\text{-}d}$ - [dioxane] relationship can be predicted by considering dioxane-water complex formation through hydrogen bonds as has been previously observed in (18,19). This non-linear relationship becomes linear again when $f_{w\text{-}d}$ is plotted against R instead of just the dioxane concentration (Figure 2c).

Despite the fact that the dioxane:water concentration was designed to be constant throughout all the lipid tubes and the surrounding fluid (15% v/v giving a predicted peak area of 0.127), small variations in the measured peak area ratio (R) were found between the different lipid tubes e.g.

between 0.105 to 0.122 (see Figures 1d and 1j). It is not clear why R was variable and slightly less than expected (0.127). If anything, one might have expected a reduction in the water peak area, giving an increased R, due to the freeze-thawing during MLV formation or due to association of water with the lipids. Plots of R against lipid concentrations (Figures 1d and 1j) show that R decreased with increasing GC (and POPC) concentration in the GC experiments (Fig. 1d) and increased with POPC concentration in one of the POPC experiments (Fig. 1j) and showed no correlation with POPC concentration in the other (not shown). A potential explanation for these effects could be some sort of differential compartmentalisation of the dioxane and/or the water so that they reside in different proportions in the three available compartments: in between the lipid bilayers, inside the MLVs or outside them. If this differential compartmentalisation of dioxane and water were to explain the different behavior of R with lipid concentration for GC+POPC MLVs and pure POPC MLVs then the compartmentalisation would then also need to be different between these two types of MLVs.

The significant dependence of the corrected f_e on POPC concentration is intriguing considering POPC has only a single exchangeable OH proton per molecule. Given that the GC MLVs also contained POPC (GC:POPC 1:2), one might conclude that GC may have an opposing (and doubly large) effect on f_e compared to POPC. This would then suggest that the effects of GC and POPC on f_e result from exchangeable protons with different chemical shifts. This implies that the magnitude of f_e may vary considerably depending on the relative concentration of particular lipid species.

A further possibility is that, in addition to the measured interactions between dioxane and water, dioxane may also interact directly with lipids, making it an even less desirable reference substance. There is some evidence that dioxane could interact with lipids as it has been used as a solvent for lipids (28-30) and has been found to disrupt hydrophobic lipid-protein interactions (31). Furthermore, the dioxane resonance frequency has been found to shift in PBS when

compared with pure water (22). Future experiments to test whether lipid-dioxane interactions could have affected these results could involve replication of the water-dioxane experiment with multilamellar vesicles present at a constant lipid concentration. If the results were significantly different from those shown here in Figures 2 and 3 then this would provide evidence for the water-dioxane interaction being affected by the presence of lipids.

In order to completely eliminate the influence of interactions between the reference chemical and the water or lipids on the results of future experiments, it would be necessary to devise a reference-chemical-free method for measuring exchange-induced frequency shifts. This is difficult to do because the primary reason for using internal reference chemicals is to allow removal of the susceptibility-induced frequency shifts. This separation of exchange-induced and susceptibility-induced frequency shifts cannot be done using an external reference or while the magnetic susceptibilities of cerebrosides and POPC are still unknown.

If a reference-free method to measure f_e shifts can be developed, it might be interesting to investigate lipid-based f_e contrast in neurological diseases as phospholipids such as POPC are a primary constituent of cell membranes and cerebrosides are essential for axonal myelin membrane integrity (32-34).

Conclusion:

Exchange-induced frequency shifts f_e were measured in MLVs formed from cerebrosides (GC) and phospholipids (POPC) developed here to model WM cell membranes. Based on a confounding effect due to unexpected small variations in the concentration of dioxane, which was used as an internal frequency reference to remove susceptibility-induced frequency shifts, we devised a method to correct the MLV data. Following this correction, a significant increase in uncorrected f_e with GC concentration was abolished and a small but significant linear increase in f_e with POPC concentration was observed: $\Delta f_{POPC} = 0.044 \pm 0.008$ ppb/mM. Straightforward

interpretation would suggest that lipids add no more than a minor contribution to f_e and, more generally, to frequency variations observed in brain tissue. However, generalizing these findings to the *in-vivo* case should be done tentatively, partly because of the difficulty in realistic modelling of the conditions encountered *in vivo* and partly because of the limitations of the method used to correct the MLV data. In addition, further research is needed to develop a reference-chemical-free method that can separate exchange-induced from susceptibility-induced frequency shifts so that the specific contributions from individual lipids can be more accurately quantified.

Acknowledgements:

We thank Dr Eugenia Poliakov and Dr Christian Wunder for extensive help with vesicle preparation and Dr Peter Macdonald for useful advice and discussions. We are grateful to Dr Doug Morris for practical assistance with chemical shift imaging experiments and useful discussions and to Stephanie French for laboratory support. We thank Dr Jacco de Zwart for computer and programming support. This research was supported by the intramural research program of the National Institute for Neurological Disorders and Stroke at the National Institutes of Health.

References:

1. Duyn JH, van Gelderen P, Li TQ, de Zwart JA, Koretsky AP, Fukunaga M. High-field MRI of brain cortical substructure based on signal phase. *Proc Natl Acad Sci U S A* 2007;104(28):11796-11801.

2. Shmueli K, de Zwart JA, van Gelderen P, Li TQ, Dodd SJ, Duyn JH. Magnetic susceptibility mapping of brain tissue in vivo using MRI phase data. *Magn Reson Med* 2009;62(6):1510-1522.

3. Mark Haacke E, Reichenbach JR, Wang Y. Susceptibility-Weighted Imaging and Quantitative Susceptibility Mapping. *Brain Mapping: An Encyclopedic Reference*. Volume 1; 2015. p 161-172.

4. Shmueli K, Dodd SJ, Li TQ, Duyn JH. The contribution of chemical exchange to MRI frequency shifts in brain tissue. *Magn Reson Med* 2011;65(1):35-43.

5. Luo J, He X, d'Avignon DA, Ackerman JJ, Yablonskiy DA. Protein-induced water 1H MR frequency shifts: contributions from magnetic susceptibility and exchange effects. *J Magn Reson* 2010;202(1):102-108.

6. Zhong K, Leupold J, von Elverfeldt D, Speck O. The molecular basis for gray and white matter contrast in phase imaging. *Neuroimage* 2008;40(4):1561-1566.

7. Norton WT, Cammer W. Isolation and Characterization of Myelin. In: Morell P, editor. *Myelin*. 2nd ed. New York: Plenum Press; 1984. p 155.

8. O'Brien JS, Sampson EL. Lipid composition of the normal human brain: gray matter, white matter, and myelin. *J Lipid Res* 1965;6(4):537-544.

9. Wennekes T, van den Berg RJ, Boot RG, van der Marel GA, Overkleeft HS, Aerts JM. Glycosphingolipids--nature, function, and pharmacological modulation. *Angew Chem Int Ed Engl* 2009;48(47):8848-8869.

10. Tan RX, Chen JH. The cerebrosides. *Nat Prod Rep* 2003;20(5):509-534.

11. Wiegandt H, editor. Glycolipids. Volume 10. Amsterdam: Elsevier; 1985.

12. Zaraiskaya T, Jeffrey KR. Molecular dynamics simulations and 2H NMR study of the GalCer/DPPG lipid bilayer. *Biophys J* 2005;88(6):4017-4031.

13. Fidorra M, Heimburg T, Bagatolli LA. Direct visualization of the lateral structure of porcine brain cerebrosides/POPC mixtures in presence and absence of cholesterol. *Biophys J* 2009;97(1):142-154.

14. Kucharczyk W, Macdonald PM, Stanisz GJ, Henkelman RM. Relaxivity and magnetization transfer of white matter lipids at MR imaging: importance of cerebrosides and pH. *Radiology* 1994;192(2):521-529.

15. Skarjune R, Oldfield E. Physical studies of cell surface and cell membrane structure. Deuterium nuclear magnetic resonance studies of N-palmitoylglucosylceramide (cerebroside) head group structure. *Biochemistry* 1982;21(13):3154-3160.

16. Leutritz T, Hilfert L, Smalla KH, Speck O, Zhong K. Accurate quantification of water-macromolecule exchange induced frequency shift: Effects of reference substance. *Magnetic Resonance in Medicine* 2013;69(1):263-268.

17. Leutritz T, Hilfert L, Smalla K-H, Speck O, Zhong K. Accurate Determination of Water-Macromolecule Exchange Independent of Reference Interaction. *Proc Intl Soc Mag Reson Med* 2011;19:4526.

18. Mizuno K, Imafuji S, Fujiwara T, Ohta T, Tamiya Y. Hydration of the CH groups in 1,4-dioxane probed by NMR and IR: Contribution of blue-shifting CH center dot center dot center dot OH2 hydrogen bonds. *J Phys Chem B* 2003;107(16):3972-3978.

19. Fratiello A, Douglass DC. NMR shift and diffusion study of dioxane-H2O and pyridine-H2O mixtures. *Journal of Molecular Spectroscopy* 1963;11(1):465-482.

20. Hope MJ, Bally MB, Mayer LD, Janoff AS, Cullis PR. Generation of Multilamellar and Unilamellar Phospholipid-Vesicles. *Chemistry and Physics of Lipids* 1986;40(2-4):89-107.

21. Shimizu A, Ikeguchi M, Sugai S. Appropriateness of Dss and Tsp as Internal References for H-1-Nmr Studies of Molten Globule Proteins in Aqueous-Media. *Journal of Biomolecular Nmr* 1994;4(6):859-862.

22. Luo J, He X, Yablonskiy DA. Magnetic susceptibility induced white matter MR signal frequency shifts - Experimental comparison between Lorentzian sphere and generalized Lorentzian approaches. *Magnetic Resonance in Medicine* 2014;71(3):1251-1263.

23. Levitt MH. *Spin Dynamics. Basics of Nuclear Magnetic Resonance*. Chichester, England: John Wiley & Sons Ltd; 2008. p 493-496.

24. Conturo TE, Smith GD. Signal-to-noise in phase angle reconstruction: dynamic range extension using phase reference offsets. *Magn Reson Med* 1990;15(3):420-437.

25. Drost DJ, Riddle WR, Clarke GD. Proton magnetic resonance spectroscopy in the brain: report of AAPM MR task group #9. *Medical Physics* 2002;29(9):2177-2197.

26. Shmueli K, Dodd SJ, Wunder C, Duyn J. Could Lipids Contribute to the Exchange-Induced Resonance Frequency Contrast in Brain Tissue? *Proceedings 20th Scientific Meeting, International Society for Magnetic Resonance in Medicine* 2011;19:704.

27. Lee J, Shmueli K, Fukunaga M, van Gelderen P, Merkle H, Silva AC, Duyn JH. Sensitivity of MRI resonance frequency to the orientation of brain tissue microstructure. *Proc Natl Acad Sci U S A* 2010;107(11):5130-5135.

28. Mukhopadhyay L, Bhattacharya PK, Moulik SP. Thermodynamics of water-induced precipitation of cholesterol and its acetate, benzoate and stearate derivatives dissolved in 1,4-dioxane and 2-propanol. *Indian J Biochem Biophys* 1989;26(5):340-342.

29. Mukhopadhyay L, Ray J, Das S, Bhattacharya PK, Moulik SP. Water-induced precipitation of cholesterol dissolved in organic solvents in the absence and presence of surfactants and salts. *Indian J Biochem Biophys* 1989;26(3):178-185.

30. Forti FL, Goissis G, Plepis AMG. Modifications on collagen structures promoted by 1,4-dioxane improve thermal and biological properties of bovine pericardium as a biomaterial. *J Biomater Appl* 2006;20(3):267-285.

31. Dees C, German TL, Wade WF, Marsh RF. Characterization of lipids in membrane vesicles from scrapie-infected hamster brain. *Journal of General Virology* 1985;66(4):861-870.

32. Boggs JM, Gao W, Hirahara Y. Myelin glycosphingolipids, galactosylceramide and sulfatide, participate in carbohydrate-carbohydrate interactions between apposed membranes and may form glycosynapses between oligodendrocyte and/or myelin membranes. *Biochim Biophys Acta* 2008;1780(3):445-455.

33. Boggs JM, Gao W, Zhao J, Park HJ, Liu Y, Basu A. Participation of galactosylceramide and sulfatide in glycosynapses between oligodendrocyte or myelin membranes. *FEBS Lett* 2010;584(9):1771-1778.

34. Bosio A, Binczek E, Stoffel W. Functional breakdown of the lipid bilayer of the myelin membrane in central and peripheral nervous system by disrupted galactocerebroside synthesis. *Proc Natl Acad Sci U S A* 1996;93(23):13280-13285.

Table 1: Concentrations of Lipids (mM) in MLV Samples with Molar Fractions (%) of all Components

Note that the final lipid concentrations (mM) in each tube after the addition of 15% v/v dioxane were equal to the values in the first three columns of the table divided by 1.15.

Concentration (mM)				Molar Fraction (%)		
Cerebrosides	POPC	Total Lipids	ROI Color	Total Lipids	Water	Dioxane
4	8	12	green	0.021	96.900	3.079
11	22	33	yellow	0.058	96.864	3.078
18	36	54	pink	0.094	96.829	3.077
25	50	75	cyan	0.131	96.793	3.076
32	64	96	orange	0.168	96.758	3.075
39	78	117	purple	0.204	96.722	3.074

Table 2: Concentrations of Water and Dioxane in the Water-Dioxane Experiment

The large outer tube was included as a data point in this experiment and contained the lowest dioxane concentration. Note that the concentration of water and dioxane in the lipid MLV experiments was nominally closest to the highlighted row in the table i.e. 15% v/v dioxane/water corresponds to a water concentration of 48,169 mM and a dioxane concentration of 1,531 mM.

Molar fraction of water	Molar fraction of Dioxane	Water concentration (mM)	Dioxane concentration (mM)
0.99	0.01	52873	534
0.98	0.02	50527	1031
0.97	0.03	48337	1495
0.96	0.04	46290	1929
0.93	0.07	40873	3076
0.90	0.10	36337	4037
0.85	0.15	30221	5333
0.80	0.20	25409	6352

Table 3: Summary of the Results of Experiments to Measure f_e in Lipid MLVs

Gradients of best-fit lines (with standard errors) for both uncorrected and corrected exchange-induced frequency shifts f_e against lipid concentration. r^2 values are also shown for the best fit lines together with p values for the mean r^2 values from a two-sided t-test.

						Corrected for Water-Dioxane Frequency Shift			
Experiment	**Repetition**	**Gradient of fe v. lipid concentration (ppb/mM)**	**SE on gradient of fe v. lipid concentration (ppb/mM)**	**r^2**	**p**	**Gradient of fe v. lipid concentration (ppb/mM)**	**SE on gradient of fe v. lipid concentration (ppb/mM)**	**r^2**	**p**
GC	1	0.208	0.027	0.937		0.023	0.046	0.058	
	2	0.208	0.027	0.935		0.023	0.032	0.111	
	Mean	**0.208**	**0.027**	**0.936**	**0.002**	**0.023**	**0.037**	**0.085**	**0.576**
POPC 1	1	0.043	0.025	0.421		0.045	0.006	0.930	
POPC 2	1	0.006	0.018	0.025		0.043	0.009	0.844	
	2	0.011	0.021	0.067		0.045	0.009	0.866	
	3	0.010	0.020	0.059		0.043	0.008	0.869	
	Mean	**0.018**	**0.022**	**0.143**	**0.460**	**0.044**	**0.008**	**0.877**	**0.006**

FIGURE LEGENDS

Figure 1. Results of Measuring f_e in Lipid Experiments

Exchange-induced frequency maps in the GC (a) and POPC (g) experiments. The exchange-induced frequency maps are scaled between -2 and +3 Hz. The magnitude images at TE = 9.6 ms are shown in figures (b) and (h) together with ROIs used to obtain the mean and standard deviation of f_e in each tube. The lipid concentrations in each tube increase from green (A lowest concentration) to yellow, pink, cyan, orange, and purple (F highest concentration) (see Table 1). The large blue ROI indicates the surrounding PBS and the black circles are air bubbles that were excluded from the ROI analysis. The graphs in (c) and (i) show the mean exchange-induced frequency in each ROI plotted against the cerebroside (c) or POPC (i) concentration in each tube. The graphs in (f) and (l) show the corrected f_e values plotted against the cerebroside (f) or POPC (l) concentration in each tube. The peak area ratios (R) measured in the GC (d) and POPC (j) experiments are plotted against the relevant lipid concentration in each tube; the value from the surrounding PBS has been added as the '0 mM' value. These values, together with the linear relationship from the best-fit of $f_{w\text{-}d}$ v. R (Figure 2c) were used to calculate a predicted additional frequency shift shown in (e) and (k) for GC and POPC respectively. The corrected values in (f) and (l) were obtained by subtracting the additional frequency shift (i.e. the frequency shift minus the intercept of the best-fit line) in (e) and (k) from the original frequency shifts in (c) and (i) respectively. In figures (c-f) and (i-l) the best-fit lines are given, together with the r^2 values. The error bars on each point indicate the standard deviation in each ROI.

Figure 2. Results of Measuring $f_{w\text{-}d}$ in Water-Dioxane Experiments

Exchange-induced frequency $f_{w\text{-}d}$ map for the different water/dioxane concentrations shown in Table 2 (a) scaled between -139 and+ 91 Hz. Peak area ratio R (dioxane:water) plotted against the inverse of the water molar fraction for the water/dioxane mixtures at different concentrations to test the predicted relationship in Equation 2 (b). The best-fit line is shown together with the r^2 value. The measured interaction-induced water-dioxane frequency shift $f_{w\text{-}d}$ for the

water/dioxane mixtures at different concentrations plotted against the measured peak area ratio R (dioxane:water) (c). The best-fit line is shown together with the r^2 value and this relationship was used together with the measured peak area ratios in each lipid tube to correct the measured f_e values in the lipid experiments. The error bars on each point in the graphs indicate the standard deviation in each ROI. Note that the total frequency difference between dioxane and water peaks would be given by the interaction-induced shift $f_{w\text{-}d}$ plotted here in addition to the expected chemical shift difference between dioxane and water (1.04 ppm) (4) and thus remains positive over the whole range of peak area ratios.

Figure 3. Results of Measuring $f_{w\text{-}d}$ v. Dioxane Concentration in Water-Dioxane Experiments

Exchange-induced frequency $f_{w\text{-}d}$ plotted against dioxane concentration (black ×s). For comparison with Leutritz et al. (16), a linear fit was performed over the four lowest dioxane concentrations giving a gradient of -0.0206 ± 0.0022 ppb/mM and $r^2 = 0.9782$. The relationship given in (19) is shown to fit the data closely: $r^2 = 0.9984$. The error bars on each point in the graphs indicate the standard deviation in each ROI therefore the point at the lowest concentration has the largest error because it came from the largest (outer tube) ROI. Note that the total frequency difference between dioxane and water peaks would be given by the interaction-induced shift $f_{w\text{-}d}$ in addition to the expected chemical shift difference between dioxane and water (1.04 ppm) (4) and thus remains positive over the whole concentration range.

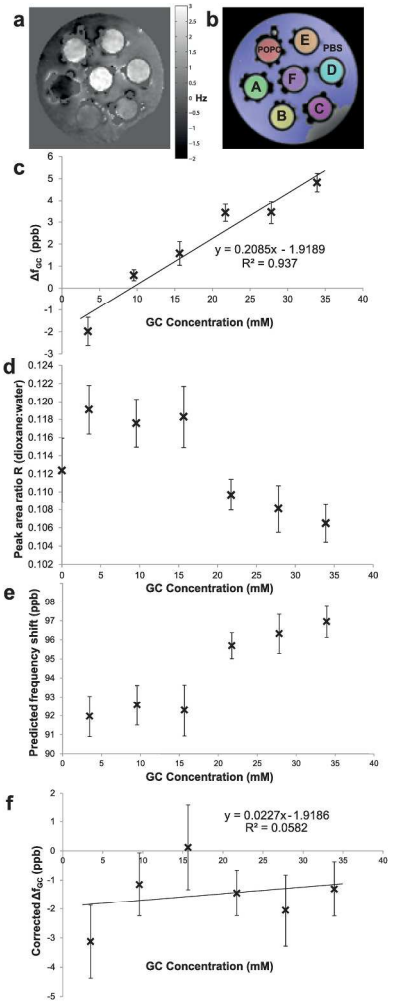

Figure 1. Results of Measuring f_e in Lipid Experiments\nExchange-induced frequency maps in the GC (a) and POPC (g) experiments. The exchange-induced frequency maps are scaled between -2 and +3 Hz. The magnitude images at TE = 9.6 ms are shown in figures (b) and (h) together with ROIs used to obtain the mean and standard deviation of f_e in each tube. The lipid concentrations in each tube increase from green (A lowest concentration) to yellow, pink, cyan, orange, and purple (F highest concentration) (see Table 1). The large blue ROI indicates the surrounding PBS and the black circles are air bubbles that were excluded from the ROI analysis. The graphs in (c) and (i) show the mean exchange-induced frequency in each ROI plotted against the cerebroside (c) or POPC (i) concentration in each tube. The graphs in (f) and (l) show the corrected f_e values plotted against the cerebroside (f) or POPC (l) concentration in each tube. The peak area ratios (R) measured in the GC (d) and POPC (j) experiments are plotted against the relevant lipid concentration in each tube; the value from the surrounding PBS has been added as the '0 mM' value. These values, together with the linear relationship from the best-fit of $f_{w\text{-}d}$ v. R (Figure 2c) were used to calculate a predicted frequency shift shown in (e) and (k) for GC and POPC respectively. The corrected values in (f) and (l) were obtained by subtracting the residual frequency shift (i.e. the frequency shift minus the intercept of the best-fit line) in (e) and (k) from the original frequency shifts in (c) and (i) respectively. In figures (c-f) and (i-l) the best-fit lines are given, together with the r^2 values. The error bars on each point indicate the standard deviation in each ROI.
296x296mm (300 x 300 DPI)

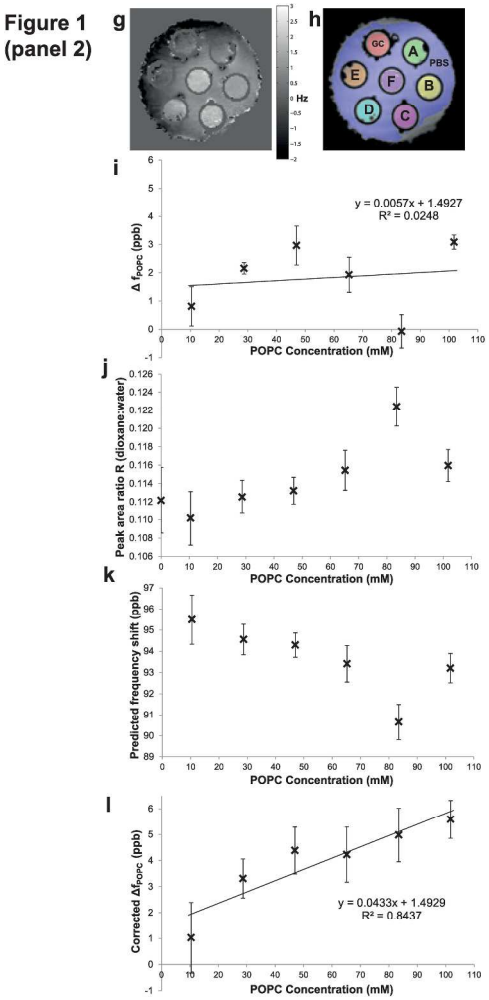

Figure 1. Results of Measuring f_e in Lipid Experiments\nExchange-induced frequency maps in the GC (a) and POPC (g) experiments. The exchange-induced frequency maps are scaled between -2 and +3 Hz. The magnitude images at TE = 9.6 ms are shown in figures (b) and (h) together with ROIs used to obtain the mean and standard deviation of f_e in each tube. The lipid concentrations in each tube increase from green (A lowest concentration) to yellow, pink, cyan, orange, and purple (F highest concentration) (see Table 1). The large blue ROI indicates the surrounding PBS and the black circles are air bubbles that were excluded from the ROI analysis. The graphs in (c) and (i) show the mean exchange-induced frequency in each ROI plotted against the cerebroside (c) or POPC (i) concentration in each tube. The graphs in (f) and (l) show the corrected f_e values plotted against the cerebroside (f) or POPC (l) concentration in each tube. The peak area ratios (R) measured in the GC (d) and POPC (j) experiments are plotted against the relevant lipid concentration in each tube; the value from the surrounding PBS has been added as the '0 mM' value. These values, together with the linear relationship from the best-fit of $f_{w\text{-}d}$ v. R (Figure 2c) were used to calculate a predicted frequency shift shown in (e) and (k) for GC and POPC respectively. The corrected values in (f) and (l) were obtained by subtracting the residual frequency shift (i.e. the frequency shift minus the intercept of the best-fit line) in (e) and (k) from the original frequency shifts in (c) and (i) respectively. In figures (c-f) and (i-l) the best-fit lines are given, together with the r^2 values. The error bars on each point indicate the standard deviation in each ROI.
301x306mm (300 x 300 DPI)

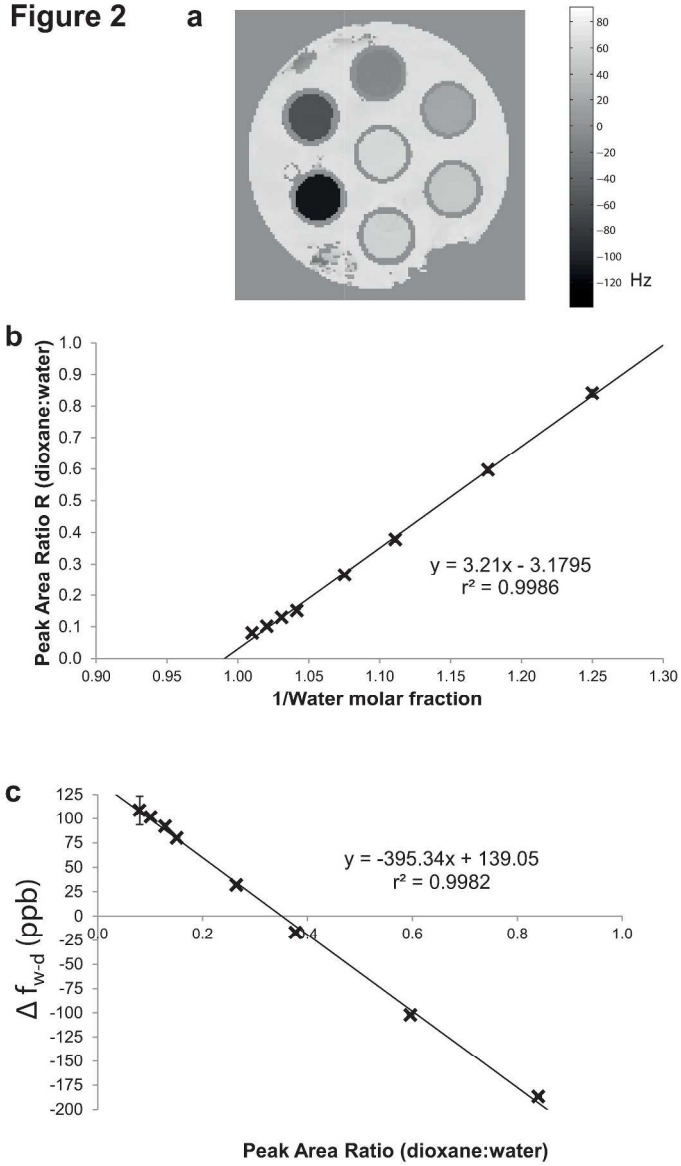

Figure 2. Results of Measuring f_{w-d} in Water-Dioxane Experiments

Exchange-induced frequency f_{w-d} map for the different water/dioxane concentrations shown in Table 2 (a) scaled between -139 and+ 91 Hz. Peak area ratio R (dioxane:water) plotted against the inverse of the water molar fraction for the water/dioxane mixtures at different concentrations to test the predicted relationship in Equation 2 (b). The best-fit line is shown together with the r^2 value. The measured interaction-induced water-dioxane frequency shift f_{w-d} for the water/dioxane mixtures at different concentrations plotted against the measured peak area ratio R (dioxane:water) (c). The best-fit line is shown together with the r^2 value and this relationship was used together with the measured peak area ratios in each lipid tube to correct the measured f_e values in the lipid experiments. The error bars on each point in the graphs indicate the standard deviation in each ROI. Note that the total frequency difference between dioxane and water peaks would be given by the interaction-induced shift f_{w-d} plotted here in addition to the expected chemical shift difference between dioxane and water (1.04 ppm) (4) and thus remains positive over the whole range of peak area ratios.

253x364mm (300 x 300 DPI)

Figure 3

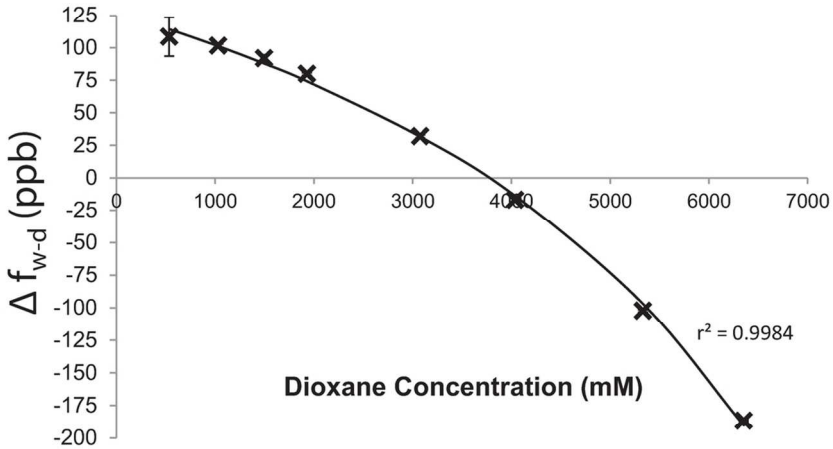

Figure 3. Results of Measuring fw-d v. Dioxane Concentration in Water-Dioxane Experiments
Exchange-induced frequency $f_{w\text{-}d}$ plotted against dioxane concentration (black ×s). For comparison with Leutritz et al. (16), a linear fit was performed over the four lowest dioxane concentrations giving a gradient of −0.0206 ± 0.0022 ppb/mM and $r^2 = 0.9782$. The relationship given in (19) is shown to fit the data closely: $r^2 = 0.9984$. The error bars on each point in the graphs indicate the standard deviation in each ROI therefore the point at the lowest concentration has the largest error because it came from the largest (outer tube) ROI. Note that the total frequency difference between dioxane and water peaks would be given by the interaction-induced shift $f_{w\text{-}d}$ in addition to the expected chemical shift difference between dioxane and water (1.04 ppm) (4) and thus remains positive over the whole concentration range.
113x80mm (300 x 300 DPI)

Graphical Abstract

Investigating Lipids as a Source of Chemical Exchange-Induced MRI Frequency Shifts

K. Shmueli, S. J. Dodd, P van Gelderen and J. H. Duyn

We measured exchange-induced frequency shifts (f_e) in a model of cell membranes consisting of multilamellar vesicles of cerebrosides and phospholipids. Using chemical shift imaging with dioxane as an internal reference to remove susceptibility-induced frequency shifts, we found significant increases in f_e with increasing lipid concentration: 0.044 ± 0.008 ppb/mM ($r^2 = 0.877$, $p < 0.01$). We also measured and corrected for the water-dioxane frequency shift which was –0.021 ± 0.002 ppb/mM dioxane in agreement with previous measurements at low dioxane concentrations.

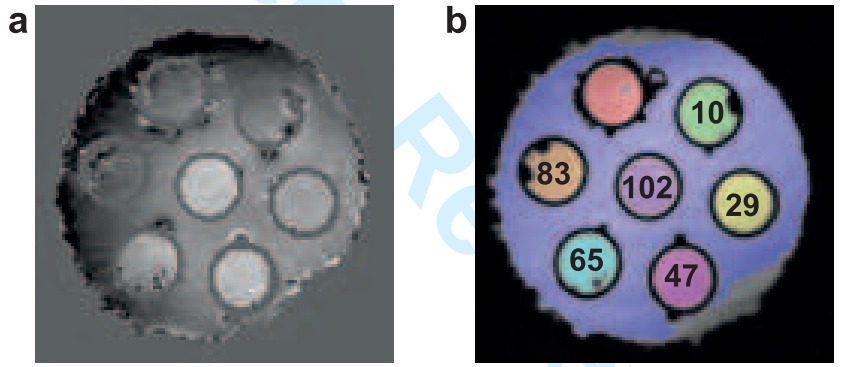

f_e map (-3.3 to 5 ppb) (a) and corrected results (c) for multilamellar vesicles with POPC concentrations (mM) in (b)

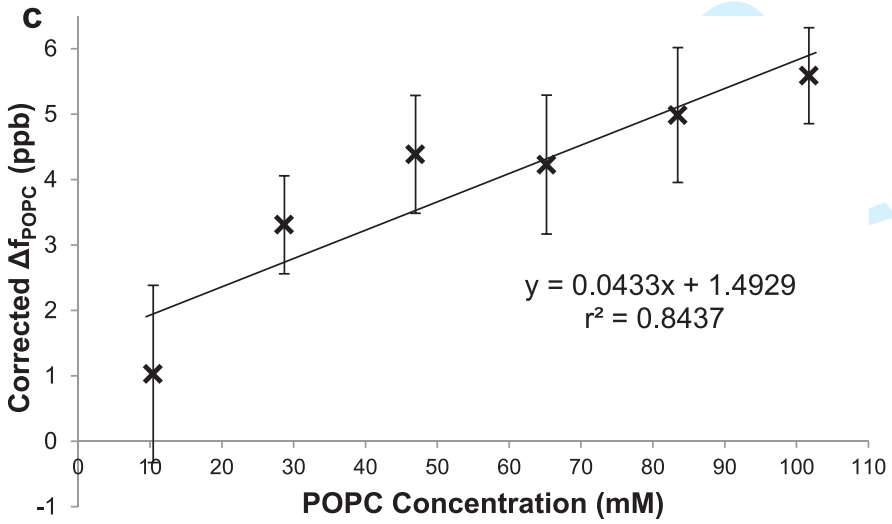

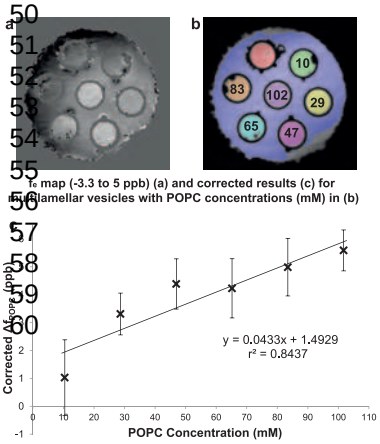

T_E map (-3.3 to 5 ppb) (a) and corrected results (c) for ELV lamellar vesicles with POPC concentrations (mM) in (b)